Reviews of Electromagnetics
Overview paper

AWE-Inspiring Electrically Small Antennas

Richard W. Ziolkowski

Abstract

Anytime-wireless-everywhere (AWE) aspirations for Internet-of-Things (IoT) applications to be enabled through current 5G and evolving 6G and beyond ecosystems necessitate the development of innovative electrically small antennas (ESAs). While a variety of ESA systems are reviewed, those realized from the near-field resonant parasitic (NFRP) antenna paradigm are emphasized. Efficiency, bandwidth and directivity issues are highlighted. Multifunctional, reconfigurable, passive and active systems that have been achieved are discussed and illustrated; their performance characteristics and advantages described. This overview finalizes by going back to the future and considers enterprising research areas of current and forward-looking interest.

Key terms

Bandwidth; directivity; efficiency; electrically small antennas; Huygens source antennas; metamaterial-inspired; metamaterials; near-field resonant parasitic (NFRP) antennas; sensors; wireless power transfer (WPT)

Global Big Data Technologies Centre, University of Technology Sydney, Ultimo 2007 NSW, Australia
***Corresponding author**: Richard.Ziolkowski@uts.edu.au

1. Introduction

The Fourth Industrial Revolution, Industry 4.0, is upon us. It represents the integration of humans and technological systems, i.e., cyber-physical systems. It promises many advances including, for instance, biometric sensors to help us maintain our health; sensor networks to enable smart infrastructure and buildings; smart agriculture to monitor crops and manage operations; autonomous vehicles to enhance our standards of living; wireless power transfer (WPT) to reduce device weight and size, eliminating short-life batteries and reducing environmental wastes; and marvelous mobile communication platforms and satellite constellations to enhance social interactions, collaborations, and cohesiveness. Electromagnetics, including antennas, propagation and measurement research, has played, is playing and will continue to play a pivotal role in realizing these anytime-wireless-everywhere (AWE) inspired dreams.

Antennas are the central technology that empowers all aspects of the Industry 4.0 wireless ecosystems, particularly those associated with the much anticipated Internet of Things (IoT) and its ubiquitous devices. Seemingly contradictory desires for radiating and receiving elements with superior multifunctional and reconfigurable performance characteristics in smaller, easier-to-fabricate and cheaper packages abound. Over 2400 journal, magazine and conference papers have been published on electrically small antennas alone in IEEE XPlore over the last decade. Needless to say, AWE-inspired electrically small antennas are an active research area for academic, commercial, and government investigators who are stakeholders in advancing wireless technologies.

This overview on electrically small antennas will begin with a brief discussion of the standard figures of merit associated with the performance characteristics of electrically small radiating and scattering systems. It will then focus on what some of the recent innovations in this area are. Systems that have overcome many of the traditional performance trade-offs associated with electrically small elements will be discussed. Novel applications benefiting from these developments and consequent future opportunities will be highlighted.

Given the ginormous number of contributions made in the ESA area by so many researchers, I will apologize up-front to all whose work is not mentioned. I will naturally emphasize the efforts associated with my group and collaborators from around the world. There are numerous books one can consult specifically for many more details on electrically small antennas, e.g., [1–3], as well as traditional antenna textbooks used worldwide, e.g., [4–6].

All of the simulations to be discussed were performed analytically (and implemented in MatLab), with in-house developed finite difference time domain software, and with commercial software environments. A majority of the antenna designs were modeled with different versions of the ANSOFT high frequency structure simulator (HFSS). More recent designs were

obtained with the corresponding HFSS tools now in the ANSYS Electromagnetics Suite. All simulations were performed with realistic materials unless otherwise noted.

2. ESA Figures of Merit

H. A. Wheeler basically provided the generally used definition of an electrically small antenna (ESA) to our technical community in 1947 [7] and later carefully clarified it in 1959 [8]. The now well-known radiansphere is the smallest sphere of radius a that completely surrounds the antenna. An electrically small transmitting or receiving antenna is one with $a < \lambda/2\pi$ or $ka < 1$. As Wheeler indicated, the radiansphere surface can be considered to be the boundary between the near and far fields of a small antenna. An associated interpretation leads to the Friis transmission equation [4, 8]. Let P_{trans} be the input power to an antenna whose effective area is A_{trans} and that is driven at the source wavelength λ. Let P_{rec} be the power received by an antenna whose effective area is A_{rec} and that is separated from the transmitting antenna by the distance r. The surface area of the sphere of radius r centered at the transmitting antenna is $S_r = 4\pi r^2$. Denoting the cross-section of the radiansphere as C_{RS}, it is given by the expression $C_{\text{RS}} = \pi a^2 = \lambda^2/(4\pi)$. Then

$$\frac{P_{rec}}{P_{trans}} = \frac{A_{\text{rec}} A_{\text{trans}}}{C_{\text{RS}} S_r} = \frac{A_{\text{rec}} A_{\text{trans}}}{\lambda^2 \, r^2} \tag{1}$$

The Wheeler cap measurement method [9, 10] in fact uses a radiation shield [8], i.e., a conducting radiansphere (hemisphere when ground plane is present) to measure the radiation efficiency of an ESA.

When most engineers hear the term "electrically small antenna", they automatically think inefficient, narrow bandwidth, minimal directivity, and a need to design an impedance matching network. Moreover, they would assume that maybe one of these performance figures-of-merit could be improved with tradeoffs amongst the others. As will be demonstrated below, these common assumptions have been proven to be no longer valid within the last two decades.

2.1. Bandwidth

In many ways the bandwidth story starts with the well-known paper by Chu [11] in which a lower-bound on the fundamental quantity, the quality factor Q, of the antenna was related to the electrical parameter, ka. The original expression was refined by McClean [12] into the generally accepted form for a passive antenna with a simple, single resonance:

$$Q_{\text{Chu}} = \left[\frac{1}{(ka)^3} + \frac{1}{ka} \right] \tag{2}$$

The seminal paper by Yaghjian and Best provided a precise discussion on how to calculate Q at a resonance (reactance is zero at f_{res} and the derivative of the reactance at f_{res} is positive) and an anti-resonance (reactance is zero at f_{res} and the derivative of the reactance at f_{res} is negative). They also related it to the derived quantity, the 3-dB fractional bandwidth (FBW), from which the generally quoted –10-dB FBW, i.e., those frequencies surrounding the simple resonance frequency with $|S_{11}| \leq -10$

dB, is readily obtained. These quantities are approximately related to Q as:

$$FBW_{3dB} \quad \sim \quad 2/Q$$

$$FBW_{10dB} \quad = \quad \frac{1}{3} FBW_{3dB} \tag{3}$$

Thus, the FBW values are essentially maximized when the lower bound on Q is achieved.

There has since been a never ending stream of reports that have attempted to define a more precise lower bound on Q. They have taken into account an antenna's geometric and other design parameters; have offered yet better understanding on how to properly calculate its reactive power; and have even incorporated time variations in its material, structural and circuit element properties, e.g, [13–22].

There are several useful rules of thumb to keep in mind that have arisen from the chatter. As has been discussed, for instance, in [23, 24], the lower bound on Q should take into account the radiation efficiency η_{rad}:

$$Q_{\text{lb}} = \eta_{\text{rad}} Q_{\text{Chu}} = \eta_{\text{rad}} \left[\frac{1}{(ka)^3} + \frac{1}{ka} \right] \tag{4}$$

i.e., the lower bound is smaller that the Chu limit. If the antenna is circularly polarized (CP) rather than linearly polarized (LP), this relation becomes:

$$Q_{\text{lb,cp}} = \frac{1}{2} \eta_{\text{rad}} \left[\frac{1}{(ka)^3} + \frac{2}{ka} \right] \tag{5}$$

These lower bound expressions point out why larger intrinsic losses and, hence, lower radiation efficiencies are acceptable in practice because larger bandwidths ensue.

Another useful improvement was derived in [13]. It was shown that the lower bound of an electric ESA with $ka \ll 1$ is more correctly $Q_{\text{lb,e}} \sim 1.5 \, Q_{\text{lb}}$ and that of a magnetic ESA is $Q_{\text{lb,m}} \sim 3 \, Q_{\text{lb}}$. Thus, an electric ESA will generally have twice the FBW in comparison to that of a magnetic ESA of similar electrical size.

Yet another important fact is that more bandwidth is accessible by a three-dimensional (3D) antenna that efficiently fills the radiansphere rather than a planar one. In fact, $Q_{\text{lb,planar}} \sim (9\pi/8) \, Q_{\text{lb}}$ [14, 17], i.e., the FBW of a planar antenna is about 3.5 times smaller than a 3D one that fills the radiansphere. There have been many studies that have suggested antenna designs that truly approach the fundamental lower bound, e.g., [23–27] A stellar example is the self-resonant four-arm spherical folded helix antenna at $ka = 0.265$ with the measured $Q = 1.52 \, Q_{\text{lb}}$ [23–25]. A review of hundreds of ESA designs in relation to the Q-based lower bound is given in [28].

Finally, defining the electrical size ka when a ground plane is present unfortunately becomes a bit nebulous. It has been shown that if the currents on the ground plane are localized near the radiator, the ground plane size has a minimal effect on

the impedance matching, e.g., [29]. Thus, the often used electrically small criterion for a radiator integrated with a ground plane, $ka \leq 0.5$, is quite reasonable. Nevertheless, it has also been shown that it fails to account for the directivity which changes dramatically depending on the size of the ground plane relative to that of the radiator [29, 30]. On the other hand, the radian sphere radius in the compilation [28] was chosen expeditiously to be the sphere which encloses the entire ground plane if its radius is smaller than $\lambda/4$, and to be the radius of the radiansphere totally enclosing the radiating elements otherwise.

2.2. Directivity and Efficiency

Directivity represents how much real power is radiated by an antenna into a particular direction when it is excited by a source relative to how much would be if the same source was driving a hypothetical isotropic electromagnetic radiator. The elemental radiators, i.e., infinitesimal electric Hertzian dipole (EHD) and loop (equivalent to a magnetic dipole) antennas are well-known to have a maximum directivity equal to $D_{max} = 1.5$ (1.76 dB) [4–6].

Electrical small radiating systems with enhanced directivity have been realized recently. These Huygens dipole antennas, i.e., balanced pairs of electric and magnetic dipole elements, have attained directivities in access of the infinitesimal system value, 3 (4.77 dB), as will be discussed more below, i.e., note that with $N = 1$ in (9), the maximum $D_{max} = 3.0$. The fact that those electrically small systems have their maximum directivity in access of this limiting value is simply due to the fact that they are finite in size and, consequently, have bits of other modes present which make small contributions to the overall radiated power.

More generally, recall that if the total radiated power is P_{rad} and the power supplied to the antenna system is P_{input}, then the total overall efficiency of an antenna would be

$$\text{Total Overall Efficiency} = 100\% \times \frac{P_{rad}}{P_{input}} \quad (6)$$

The radiation efficiency is then

$$\text{Radiation Efficiency} = 100\% \times \frac{P_{rad}}{P_{accepted}} \quad (7)$$

where the total power accepted by the antenna is $P_{accepted} = (1 - |S_{11}|^2) P_{input}$. The better matched an antenna is to its source, the more power it has to potentially radiate.

If the radiating system has an effective transverse area A_{eff} and if it is uniformly driven at the excitation wavelength λ, then its maximum directivity and realized gain are [4]

$$
\begin{aligned}
D_{max} &= \frac{4\pi}{\lambda^2} A_{eff} \\
RG_{max} &= e_{total} \times D_{max}
\end{aligned}
\quad (8)
$$

where the total efficiency of the radiating system, i.e., taking into account the material losses, mismatch losses, ..., is e_{total}. Consequently, a larger effective radiating aperture will provide a higher directivity. Moreover, these relations clearly indicate that an ESA, by nature, is directivity challenged. Note

that $e_{total} = (1 - |S_{11}|^2) e_{em}$, where the term e_{em} represents the overall efficiency associated with the radiator (all of the efficiencies tied to losses other than the mismatch loss) and, hence, the accepted power. Therefore, the maximum gain is $G_{max} = e_{em} \times D_{max}$. At a given frequency, the gain of a time-harmonic (continuous wave, CW) antenna on transmit and receive is identical.

Is there a means to achieve directivities well beyond the dipole values with a single radiator? By taking into account both the transverse electric and magnetic modes, Harrington demonstrated that the maximum directivity from a source region as a function of the maximum number of multipole modes, N, that it can radiate is [31], [32]:

$$D_{max} = N^2 + 2N \quad (9)$$

Therefore, by exciting many higher order modes, one can in principle achieve very high maximum directivity from a single element. There has been much interest recently in the physics literature to use high permittivity dielectrics to enable the overlap of dipole and higher order modes in nano-systems to attain high directivity. A Huygens nanoparticle laser based on this concept was reported in [33].

Another approach, in principle, is a superdirective system. A useful operational definition of superdirectivity, e.g., as emphasized by Hansen [34], [35], is to achieve a directivity greater than that obtained with the same antenna configuration being uniformly excited (constant amplitude and phase). While this is basically an array definition, a precise one for a single element is a bit stickier because even a tiny ideal electric Hertzian dipole is "superdirective" by it, i.e., because its directivity is 1.5, its effective electromagnetic area from (8) is $A_{eff} = 3\lambda^2/8\pi$ which is much larger than its physical area. The concept of superdirectivity has permeated the physics and applied physics literature repeatedly since Oseen discussed the concept of "needle radiation" nearly a century ago [36] and continues to be an active research field [37]. Nevertheless, it is extremely challenging in practice. There have been and continue to be many attempts to overcome the ill-posedness associated with superdirectivity, especially taking into account system constraints e.g., [38, 39]. A superdirective electrically small radiating system was recently reported in [40] based on a metamaterial-inspired multilayered nanoparticle.

3. Overcoming Conventional ESA Stigmas and Trade-offs

As noted above, experimentally verified examples of ESAs that have overcome the conventional wisdom of their drawbacks have been reported. Many were initially associated with the concept of electromagnetic metamaterials [41–43], artificial materials whose electromagnetic properties can be designed to have properties not attainable with naturally occurring media. Many more recent examples have arisen from the fundamental electromagnetic physics and engineering principles they imbue.

3.1. Metamaterial-based ESAs

The adaptation of a variety of epsilon-negative (ENG), mu-negative (MNG), and double negative (DNG) metamaterials

(MTMs) to achieve miniaturized antennas followed immediately after the initial surge of publications investigating their exotic physics properties. There are several review papers available with extensive reference lists that cover many of the designs in the first MTM decade [44–49]. I simply call your attention to several small metamaterial-based antennas reported by some of the early research teams in this area: [50–68]. Small communications and cross-dipole antennas were reviewed, respectively, in [69] and [70]. A variety of compact CRLH-based antenna systems have been reviewed very recently [71, 72], as have antennas augmented with meta-structures, e.g., [73–77].

My team's initial metamaterial-based ESA concept consisted of a center-fed electrically small dipole antenna centered in and surrounded by either a DNG [50] or an ENG [51] shell. For simplicity, I will denote it as a core-shell antenna. The driven dipole radiator is a highly capacitive element. The double positive (DPS) air region itself acts as a capacitive element. The ENG shell, for example, is also electrically small and is excited by the fields radiated by the dipole. Consequently, it too is a capacitive element. However, because it is filled with a negative permittivity medium, it acts like an inductor. The combination of the capacitive and inductive elements forms an electrically small LC resonator. Nearly complete impedance matching to the source without any matching network and radiation efficiencies approaching 100% by properly tuning them together was demonstrated [51]. It was later proved that the driven element does not have to be surrounded by the ENG shell. The consequent electrically small LC resonator formed by it and the ENG shell is strongly excited by the driven dipole as long as the dipole is in close proximity to it [78]. The basic principles of this core-shell antenna concept were verified experimentally with the dual structure, a coax-fed semi-loop antenna surrounded by a MNG hemisphere on a ground plane [79].

It must also be emphasized that there were many in the IEEE Antennas and Propagation (AP) and Microwave Theory and Techniques (MTT) professional societies who were adamant that many of these metamaterial-based concepts were not credible, even despite existing experimental results. Monographs were even published by well-known colleagues labeling some of the work as "voodoo science" or the materials with exotic and even simple properties (e.g., empathically denying the existence of media with negative parameters) as "unobtainium" [80, 81]. Some negative feelings still persist because, like many persisting and emerging areas, e.g., magnetic fusion, graphene, quantum computers, ..., there is much hype about the potential outcomes to acquire recognition and funding. Others who have jumped on the bandwagon have misused the terminology and, unfortunately, have nurtured them.

We must all understand and continue to be reminded that it really does take years to properly vet innovative ideas and truly demonstrate their unique advantages over existing systems. For instance, it was suggested that the dipole-ENG shell system could be realized based on a Drude model of a plasma in a glass shell whose density was small enough that the operating frequency of the driven dipole was below its plasma frequency. Analytical and numerical models [82, 83] suggested this approach was realistic. More than a decade later, the concept has been verified with some outstanding experimental efforts [84].

As a historical side note discussed in [85], my team and collaborators had considered passive and active materials constructed with artificial molecules before the turn of the century. As they would be currently termed, these passive and active "meta-atoms" were developed as complex passive and active loads connected to very electrically small dipole and loop antennas [86–91]. The fields re-radiated, i.e., scattered, by these designed electric (magnetic) inclusions in a substrate superimposed to yield a variety of dispersion engineered permittivity (permeability) responses. Over a decade later, the electric (meanderline antenna loaded with an inductor and magnetic (loop antenna loaded with a capacitor) unit cells shown in Fig. 1 were successfully combined into one of the electrically smallest DNG unit cells still today and a block of the resulting low loss DNG metamaterial was tested. The results experimentally verified their simulated performance characteristics [92, 93], i.e., a refractive index $n = -3.1$ with less than 1.0 dB/cm loss at 400 MHz with unit cells whose overall size was $\sim \lambda/75$.
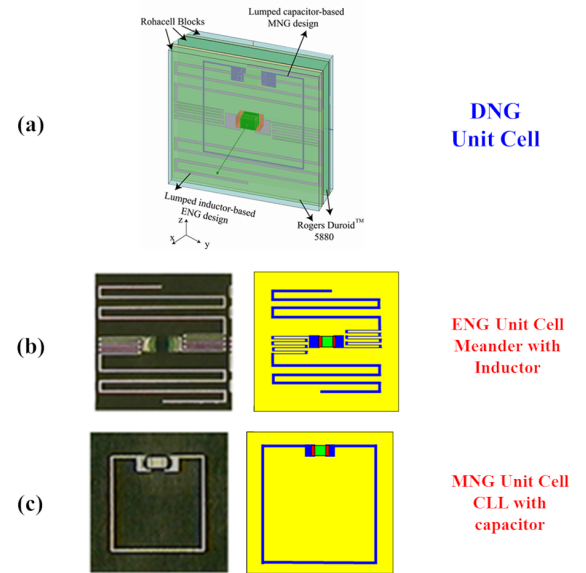

Figure 1: DNG Metamaterial with $n_{real} = -3.1$ at 400 MHz [92, 93]. Top: isometric view of the composite DNG unit cell. Middle: Meanderline antenna-based ENG layer of the unit cell. Left: photo, Right: Simulation model. Bottom: Capacitively-loaded loop (CLL) antenna-based MNG layer of the unit cell. Left: photo, Right: Simulation model.

Finally, I would be remiss not to highlight one of the first metamaterials, i.e., artificial magnetic conductors (AMCs), that were developed to enhance the performance of antennas. The high-impedance surface (HIS) mushroom [94] and UC-PBG [95] structured ground planes mitigated surface wave effects and facilitated low-profile antenna systems. Many antennas using these and other structured ground planes are nicely reviewed in [96]. An AMC based solely on CLL unit cells without the presence of a ground plane [97] realized the magnetic wall

considerations in [86]. One of the first investigations on how long in time it takes for a metamaterial to realize its properties employed a related CLL-based AMC [98]. Similar time domain considerations facilitated the realization of a zero-index metamaterial superstrate [99] for a high-gain antenna in a 60 GHz high-data-rate system. Predicted multi-Giga-bit information transfer based on an on-off-key (OOK) modulation was confirmed experimentally [100].

An electrically small NFRP antenna system that used a structured ground plane to achieve a high directivity was designed in [101]. However, we found it a severe challenge in general to fit the required periodic structure within in a Wheeler sphere smaller than $ka = 1.5$. As a consequence, we turned to other approaches to attain higher directivity ESAs as will be illustrated below.

3.2. Metamaterial-inspired ESAs

Even though very small unit cells were realized, a metamaterial, i.e., a block of artificial material consisting of enough layers of these unit cells in the wave propagation direction to attain homogenized values of the permittivity and permeability (basically 3-5) is still quite thick if one desires an antenna system that has its $ka = 0.5$, i.e., $a \sim \lambda/12.6$. Moreover, the unit cells were planar; contained lumped elements; and redesigning them for a curved geometry, e.g., the core-shell antenna system, was and remains very challenging. The three-dimensional lego-design used in [79] was bulky, and we found that precise registration (alignment) of the elements in the various layers was required for the best performance. Nevertheless, other teams successfully combined a single layer of metamaterial unit cells both as substrates and superstrates, which would now be denoted as metasurfaces, with radiating elements for enhanced performance characteristics [53,59,61].

Luckily, a paradigm shift associated with the metamaterial-based ESAs and ESAs in general arose from those efforts with the antennas reported in [102]. We found that exciting only a single metamaterial unit cell that was resonant near the operating frequency of interest with a small driven element was sufficient to achieve a highly efficient ESA without the need for any matching network. Because no metamaterial was involved, but its success followed from metamaterial designs, we coined the term "metamaterial-inspired" to denote those original ESAs. Many of the original metamaterial-inspired designs were reviewed in [44]. There have been numerous metamaterial-inspired ESAs recently reported, e.g., [103–110].

As they were investigated further, it became clear that the fundamental radiation physics and engineering of the original designs is best captured with the designation: near-field resonant parasitic (NFRP) antennas. The NFRP antennas consist of a simple driven element and one or more NFRP elements. The concept is illustrated in Figs. 2(a) and 2(b) with field and circuit concepts, respectively. By adjusting the sizes and shapes of the driven and NFRP elements, as well as the distance and material between them, one can engineer the imaginary part of the antenna's input impedance, i.e., its reactance, to be zero and its real part, i.e., its resistance, to be matched to that of the source, as well as emitting fields that are well matched to the impedance of free space. Nearly complete impedance matching
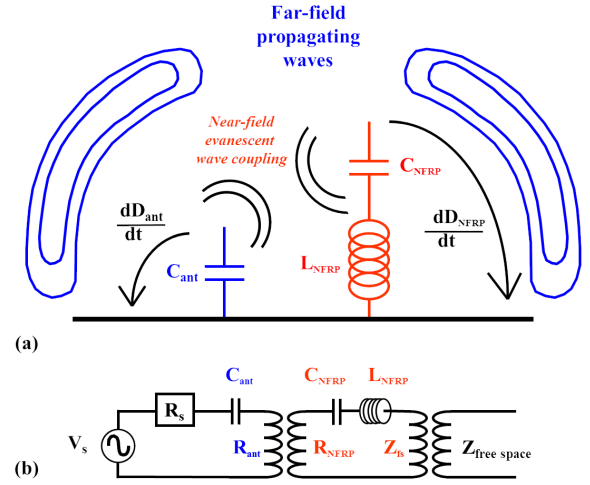

Figure 2: Fundamental operating principles of NFRP antennas [44]. (a) Electromagnetic concepts. (b) Equivalent circuit aspects.

and a high radiation efficiency are thus attained [44].

A simple example is shown in Fig. 3(a). The driven element is a small curved top-hat dipole radiator; the NFRP element is an Egyptian axe dipole (EAD) [101]. The surface currents on the driven and NFRP elements illustrated in Fig. 3(b) illustrate one of the advantages of the design, i.e., the main radiating currents occur primarily on the NFRP element, not the driven one. This aspect allows for the presence of more NFRP elements to achieve multiple functions with only a single driven element.
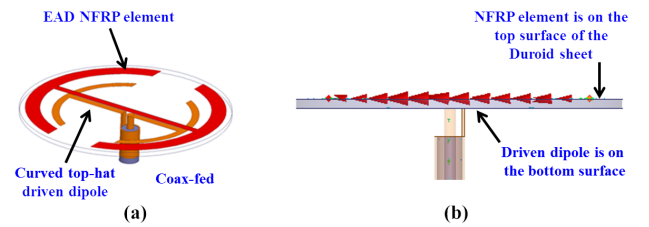

Figure 3: Egyptian axe dipole (EAD) NFRP antenna [101]. (a) HFSS model. (b) Simulated surface currents.

Two of the early NFRP antenna designs and their prototypes serve as a prelude to more recent examples. They were developed during a DARPA sponsored Multidisciplinary Research Initiative (MURI) program that was led by the Boeing Aerospace Company [85]. Boeing Phantom Works fabricated our designs and they were tested at the National Institute of Standards and Technology (NIST) in Boulder CO.

The Z-antenna shown in Fig. 4 is an electric NFRP design. A coax-fed printed monopole acts as the driven element. The inductor loaded Z structure is the NFRP element. The design served several purposes at the time. It demonstrated the flexibility to realize versions as small as $ka = 0.046$ at VHF to UHF frequencies; the ability to tune the resonances of one de-

sign over a very large bandwidth, i.e., to demonstrate frequency agility; and to understand how the overall efficiency of this type of antenna varied, for example, when ka was varied by almost an order of magnitude, i.e., from 0.016 ($\sim$ 30%) to 0.14 ($>$ 90%) [111]. Prototypes of the UHF designs were fabricated and tested [44, 112]. They were quite valuable since they taught us how to tailor the parameters to account for the lumped element being introduced into the NFRP element rather than into a circuit. The 570 MHz, $ka = 0.40$ design shown in Fig. 4 had an measured overall efficiency greater than 80%.
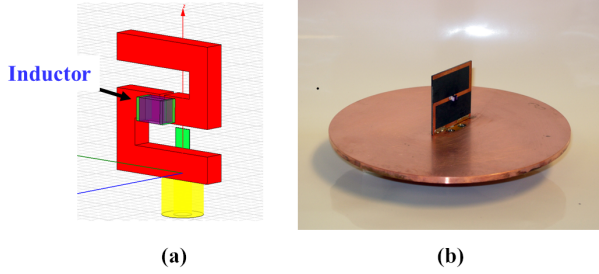

(a)   **(b)**

Figure 4: Electrically small Z-antenna. (a) HFSS model. (b) 300 MHz Prototype. [112]

The 3D magnetic EZ antenna shown in Fig. 5 was a magnetic NFRP antenna. The driven element was a coax-fed semi-loop. The NFRP element was an extruded, 3D CLL structure. Prototypes of the original design [102] were fabricated for operation at the UHF frequency of 300 MHz [44, 113] and at the VHF frequency of 100 MHz [44, 114]. The former, which had $ka \sim 0.43$ at 301 MHz, had a measured overall efficiency greater than 94%. The latter is shown in Fig. 5. It was a low profile antenna (height = $\lambda/25$) whose measured resonance frequency was 105 MHz giving $ka = 0.46$ and whose measured overall efficiency was $\sim$ 95%. The change in the radiation efficiency as ka decreases was also studied [114]. It was found in analogy with the lower bound in Q that the radiation efficiency of the magnetic NFRP designs decreased much more quickly as ka did in comparison to the their electric counterparts. Variations of this 3D magnetic EZ design has proven to be quite resilient as an ESA for high power microwave (HPM) systems [115–117].
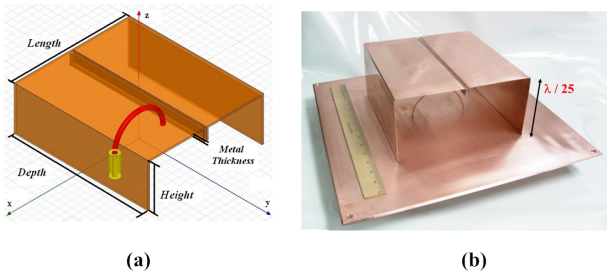

(a)   **(b)**

Figure 5: Electrically small 3D Magnetic EZ antenna. (a) HFSS model. (b) 100 MHz Prototype. [114]

The VHF and UHF systems were examined because achiev-

ing physically tiny, highly efficient antennas in those bands and even lower ones might have enabled a host of applications. A $\lambda/2$ dipole antenna at 30 MHz is approximately 5.0 m in length. Very interesting robust communications concepts have been reported recently at the lower end of the VLF band [118] among mobile agents such as robots in complex non-line-of-sight indoor and urban-type scenarios. The need for efficient miniature antennas has driven the realization of several unique designs [119–126].

3.3. Non-Foster Circuits

Recalling the lower bounds on Q for passive ESA systems, their bandwidths are naturally narrow. Most of the described early electric- and magnetic-based NFRP ESA systems exhibited fractional bandwidths on the order of 3-4% and 1-2%, respectively, in sync with those bounds. Despite the general demand for greater bandwidth, there are many narrow band antenna applications for which ESAs are well-suited. They include, for instance, the low frequency ESAs for communications between mobile agents in complex environments noted above [118] and for wireless power transfer (WPT) involving dedicated transmitters, which will discussed below. Furthermore, in conjunction with the rapid growth of the Internet of Things (IoT) applications, low power wide area networks (LPWAN) and their associated technologies, such as LoRa and Sigfox, have become popular for low-rate (narrow bandwidth) long-range radio communications [127]. LoRa systems are important for rural settings and have promising potential for search and rescue applications [128]. Nevertheless, there is always the demand for greater bandwidths in compact wireless devices.
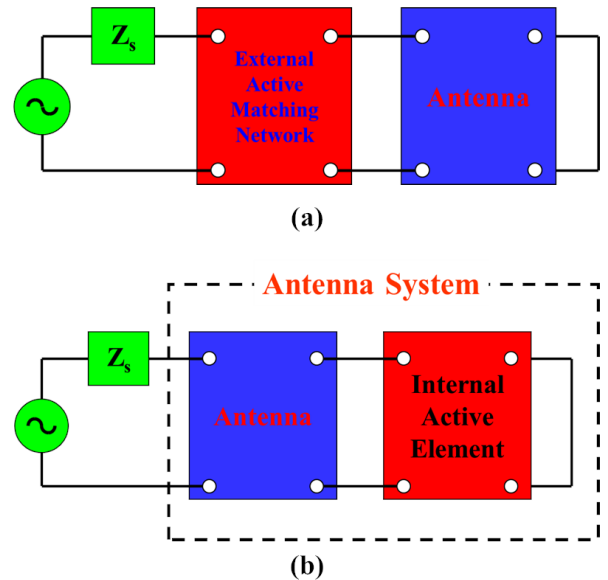

(a)

(b)

Figure 6: Methods to obtain an ESA with a large instantaneous bandwidth. (a) Active matching network. (b) Internal active element.

Because the noted physics-based bounds on Q are directly

connected to passive radiating systems, an approach to achieve a large instantaneous bandwidth with an ESA is accomplished by introducing active systems. There are two basic approaches as illustrated in Fig. 6. The first is to introduce an external active matching network that compensates for both the resistance and reactance of the input impedance of the ESA to match it to the source. The second introduces an active internal reactance element into the antenna itself. Both methods can be facilitated by using non-Foster elements, i.e., powered transistor-based circuits whose impedance characteristics can decrease with increasing frequency in violation of Foster's Reactance Theorem [129, 130]. Foster's theorem basically tells us that the stored electric and magnetic field energies of a passive electromagnetic system must remain positive as the frequency changes, i.e., the frequency derivative of its reactance must be positive. Non-Foster (NF) elements can exist because their power source introduces energy into the system, negating the passive bounds.

There have been a number of successful realizations of wide bandwidth ESAs employing both types of active approaches. External active matching networks have been considered over the last 50 years [131–144]. More recent variants recognize that the Chu bound arises from the fact that passive antennas are LTI (linear time-invariant) systems. A variety of non-LTI (active) systems have been considered to attain wider bandwidths from electrically small systems. As argued in [21], the use of non-linear and time-varying components has a long history back to first wireless telegraphy experiment in 1902 by Marconi which was successfully enabled by a spark-gap ESA. Impedance modulation, usually through the use of time varying inductor and capacitors [145], is a form of parametric amplification (see, e.g., [146], Chap. 11). This time-variation concept is also a fundamental aspect of space-time, time-modulated, and magnetless non-reciprocal metasurfaces to control radiated wavefronts and directional beams [147–153]. Another approach is the use of temporal modulation of the matching network, e.g., through the introduction of switches for direct amplitude modulation (DAM) of an ESA [154–157]. On the other hand, the internal (embedded) active elements have been reported only in the last decade [139, 158–174].

The process that my team and collaborators has used to achieve a NF-augmented NFRP antenna emphasizes the initial choice of a highly efficient, frequency-agile, passive NFRP antenna that has either an inductor or capacitor incorporated into its NFRP element(s) and has as low a Q value as possible. The presence of such a lumped element facilitates the frequency agility, i.e., it allows the antenna's resonance frequency to be tuned. Since such a low-Q passive radiator will have a wider bandwidth, it relaxes the demands on the active element's required performance.

Sweeping the lumped element's value allows one to obtain a reactance versus resonance frequency (X-f) curve and it will have a NF behavior, i.e, a negative slope with respect to the frequency. A negative impedance convertor (NIC) based on a pair of cross-coupled transistors is then designed to create an active inductor or capacitor that replaces the passive one and matches the X-f curve. The NFRP antenna design with this active element being present is further refined with a co-design process. It is critical that realistic lumped element models and all interconnecting traces in the NIC circuit implementation with the NFRP element be included in the co-design process to account for the parasitic capacitances, inductances, and resistances associated with them. The final optimal design should have the resistance of the non-Foster element as small as possible across the entire extended bandwidth to maintain the high radiation efficiency of the passive design.

Several frequency agile versions of the basic CLL-based protractor NFRP antenna [44] have been obtained and their prototypes tested [175–177]. This magnetic dipole type of NFRP antenna has been an attractive choice in practice because one can incorporate a varactor into its NFRP element, e.g., across its gap, and tune its resonance frequency simply by changing the voltage applied to the varactor. This choice was encouraged because of the successful use of varactors for tunable magnetic metamaterial unit cells in the physics literature, e.g., [178]. The analysis, simulation, and testing of the NIC-capacitor augmented version was described in the articles [159, 161, 163].
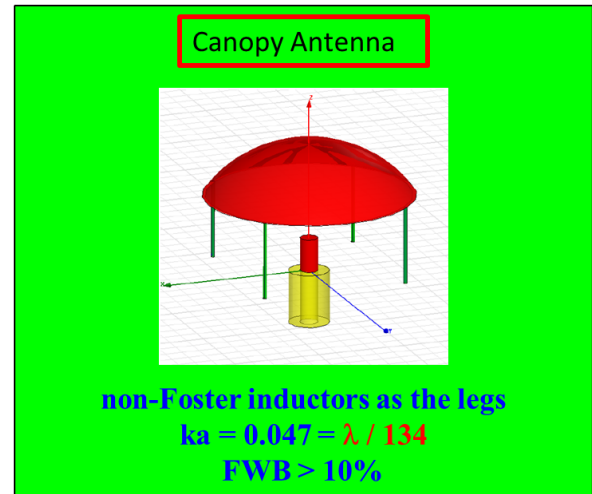

Figure 7: The canopy antenna augmented with four non-Foster elements, which are the four NIC-based inductor posts that support the metal canopy [158].

Nevertheless, the first NF-augmented ESA design we developed was actually an electric one, the canopy antenna [179]. Its structure is illustrated in Fig. 7. The NFRP element is the metallic spherical cap connected to a ground plane by four inductor posts. It is excited by the coax-fed monopole. The electric choice was associated with the noted fact that passive electric dipole based ESAs naturally have more bandwidth than the magnetic ones. Moreover, of the various electric-based NFRP ESAs considered in [179], the Q value of the canopy design came closest to the Q lower bound. The electrical size was purposely picked to be small, i.e., $ka = 0.0467$ ($a \sim \lambda/137$), for a 297.4 MHz operating frequency. The passive design had $Q = 1.75$ $Q_{\text{Chu,lb}} = 1.17$ $Q_{\text{Thal,lb}}$ and a $FBW_{10dB} = 0.0133\%$. Replacing the passive inductors with NIC-versions, the FBW was greater than 10% [158]. This stellar result actually encouraged the subsequent NIC-inductor augmented EAD-based NFRP ESA prototypes [159, 160, 163], one of which is shown in Fig. 8(a). The measured results confirmed a bandwidth several times the

fundamental passive upper bound. Similar outcomes have been reported with embedded NF elements in [166, 167].

Performance comparisons of the two-dimensional (2D) NF EAD version in Fig. 8(a) and a three-dimensional (3D) variation were considered in [168]. The results confirmed that initial passive antenna designs that have wider instantaneous bandwidths (i.e., smaller Q values), regardless of their 2D or 3D nature, will perform better than narrower bandwidth ones when they are augmented with the NF elements. This outcome is due to their decreased sensitivities to component and fabrication tolerance errors encountered with the NF circuit realizations. The recently tested 3D CLL-based NIC-capacitor augmented magnetic NFRP ESA shown in Fig. 8(b) further confirmed these conclusions [173].
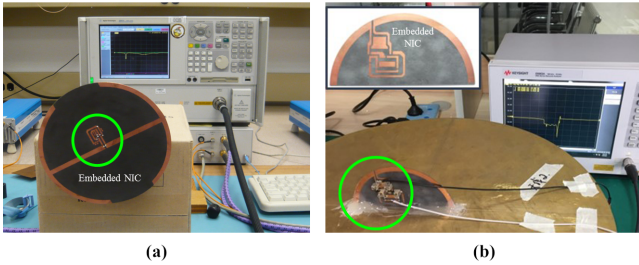

(a)   (b)

Figure 8: Experimentally validated NFRP ESAs whose NFRP elements were augmented with non-Foster elements. (a) EAD example (NIC-inductor) [160]. (b) CLL example (NIC-capacitor) [173].

Despite the promising results from both the internal and external NF approaches, many challenges remain. Many of them are nicely reviewed in [180]. In particular, it is well known that the cross-coupled transistor realizations, for instance, of NIC elements depend on positive feedback for their operation and, hence, are very prone to instabilities. Stability analyses [136, 181–183] have led to further understanding of the appearance of NIC instabilities and their mitigation. Moreover, the NIC designs are very sensitive to the actual parameters of the physical components used to realize them, as well as to their assembly with manual soldering. A very promising method that avoids component tolerance and assembly issues is to realize the NIC element as a complementary metal–oxide semiconductor (CMOS) processed integrated circuit (IC) [184–186]. Another attractive approach recently reported is to not avoid the instabilities, but to use them to power the radiating elements as self-oscillating antennas [187]. The initial prototype crossed [187] and Huygens [188, 189] dipole self-oscillating antennas have significantly wide measured frequency-agile impedance bandwidths.

Yet another performance issue with active elements, particularly in a receiving antenna, is the signal-to-noise-ratio (SNR). There have only been a few investigations reported. Both [190] and [191] consider the active matching circuit approach. While the former indicates that there may be NF advantages overall, the latter concludes there are none. In contrast, the internal NF element approach SNR study [173] with the 3D NF CLL-based ESA shown in Fig. 8(b) demonstrated significant improvements.

More studies will need to be performed to attain a conclusive answer in general if there is one. Again, because of the active nature of the systems, the SNR outcome may simply depend on the NF element design and how it is employed.

4. More Complex Electrically Small NFRP Antennas

One of the advantages of the NFRP ESA paradigm is that it facilitates incorporating several NFRP elements within an electrically small volume. Because the NFRP elements are not connected directly to the source in any way nor necessarily with each other, the function that each one performs can be developed (in many cases) completely independent from the others. Multifunctional ESAs are an immediate consequence. They are, of course, quite advantageous in many wireless applications desiring more capabilities in ever smaller footprints. Moreover, this separation of intended functions allows one to incorporate additional electronic components that are associated with either the driven or NFRP elements or both. This additional degree of design freedom allows one to achieve a variety of reconfigurable ESA systems.

4.1. Multifunctional Designs

A few of the earlier NFRP designs illustrate the multifunctional concept in an electrically small package. By introducing two orthogonal electric NFRP elements of different sizes and a bowtie-shaped driven element that excites both of them, linear polarized (LP) fields at two independent frequencies of operation, GPS-L1 and Global Star (GS), were obtained in [192]. Moreover, CP fields were also obtained at a specified operating frequency f_0 with the same configuration without any phase shifter simply by adjusting the NFRP element shapes and sizes to have one resonance slightly above f_0 and one below it so their reactances naturally provide the requisite 90° phase difference between the LP radiators. A three metal layer, dual-band CP version also made good use of the crossed-dipole resonator configuration [193]. All had high radiation efficiencies.

The two resonator design was extended to four resonators in [194] to obtain CP fields radiated at the GPS-L1 and GPS-L2 frequencies. The tested prototype is shown in Fig. 9(a). Four interleaved magnetic-based protractor NFPR elements were driven by two printed monopoles fed with a single coax. The electric resonator concept was further extended to eight elements in [195]. The optimized design parameters of this compact structure were determined to naturally obtain CP radiation and multi-band operation that covered all five of the GPS bands, L1–L5. The tested prototype is shown in Fig. 9(b).

Other multi-band NFRP ESAs have also been developed. These include monopole [196] and dipole driven [197] elements loaded with CLL NFRP elements as their resonators. Integrating an AMC surface with pairs of crossed-dipole resonators, a tri-band CP antenna was achieved [198].

Filtennas are another multifunctional antenna concept that leads to more compact front-ends in wireless communication systems. They represent the advantageous integration of the filter(s) with the antenna into a single module. They possess attractive features such as a controllable passband frequency
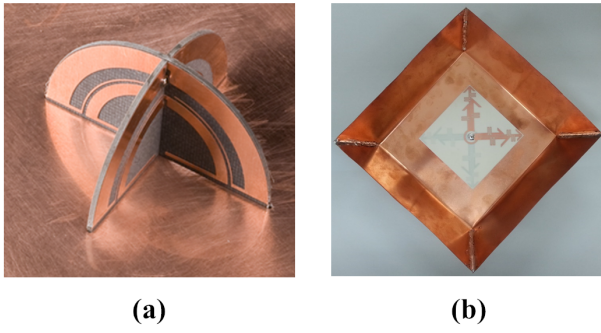
(a)   **(b)**

Figure 9: Experimentally validated multifunctional NFRP ESAs. (a) Four resonators for dual-band CP operation. [194]. (b) Eight resonators to obtain CP operation at all five GPS frequencies, L1-L5 [195].

response in both their reflection coefficient and realized gain values. They have become popular for the next generation of wireless devices supporting high-speed data rates and portable applications [199]. Electrically small filtennas that have relied on CLL-based resonators [200], more complex driven elements to attain LP radiation [201], and more complicated NFRP elements to achieve more bandwidth for both LP and CP performance [202].

4.2. Reconfigurable Designs

Reconfigurable antennas are now a standard means to achieve multifunctional performance in wireless mobile terminals [203, 204]. Innovative technologies have advanced their capabilities [205]. Nevertheless, achieving reconfigurability in an electrically small package remains a challenge.

Several reconfigurable NFRP ESAs have been developed. Systems that change both pattern [206–211] and polarization [212] characteristics have been investigated. The NFRP paradigm has been particularly advantageous because the switches can be placed either in the driven elements or in the NFRP elements.

Two examples are illustrated in Fig. 10. The pattern reconfigurable ESA [208] shown in Fig. 10(a) radiates three unidirectional beams along the horizontal plane into separate 120° sectors with beamwidths completely covering each of them. The driven element is fixed. Diodes are embedded in the electric and magnetic NFRP elements and are switched on and off to direct the beam into the desired sector. Thus, this ESA provides coverage of the entire azimuthal plane.

The polarization reconfigurable ESA [212] shown in Fig. 10(b) has its NFRP elements fixed. The diodes are incorporated into its driven element. It radiates unidirectional fields in the broadside direction. Depending upon the ON and OFF states of the diodes, it radiates one of four polarization states: one of two LP states along two orthogonal planes and either LHCP (left-hand circular polarization) or RHCP (right-hand circular polarization) states.
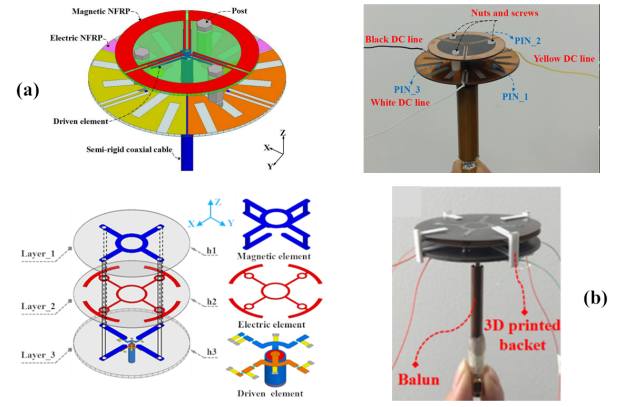

Figure 10: Experimentally validated reconfigurable NFRP ESAs. (a) Pattern reconfigurable ESA whose unidirectional 120° sector beams point along the azimuthal plane [208]. (b) Polarization reconfigurable ESA that can radiate four different polarization states: two LP and two CP [212].

5. Directive Electrically Small NFRP Antennas

As noted above, electrically small electric and magnetic dipole antennas have a directivity near to 1.5 (1.76 dB). More importantly for the following discussion, they radiate a figure-eight pattern in one principal plane with its null directions being along the dipole's axis and an omnidirectional pattern in the orthogonal one. An ESA that would radiate primarily into one hemisphere rather than both, i.e., that would have a high front-to-back ratio (FTBR), would have many advantages for applications in which maximizing the power radiated (received) towards a receiver (from a transmitter) is desirable. For instance, as a transmitter, it would not waste half of its radiated power in an unwanted direction. Moreover, if this could be achieved without the necessity of a ground plane, an antenna engineer would have more flexibility in integrating the antenna system with a mobile platform. For instance, while a monopole antenna with a finite ground plane has an omnidirectional pattern about it, its peak direction is significantly elevated from it. An NFRP ESA such as the one shown in Fig. 10(a) does not have a ground plane to finesse. Its peak is along the horizontal plane and it has a high FTBR with respect to the selected beam direction.

The two main approaches to achieving higher directivity with a NFRP ESA have been the use of a quasi-Yagi configuration in which a NFRP element acts as a director and/or another acts as a reflector. The other is by engineering a Huygens source, i.e., by arranging the driven element is manner that it effectively excites a balanced pair of in-phase electric and magnetic NFRP elements. Both approaches have achieved unidirectional endfire and broadside radiating sources.

5.1. Quasi-Yagi

The quasi-Yagi ESAs come in two main styles, 2D and 3D. For instance, the 2D version [213] is printed on a single copper-clad substrate. While it had a modest directivity, it was flexible. Its prototype was tested successfully in two bending modes and on

cylinders of different radii.

The 3D versions have quite different arrangements. A spiral-shaped driver and director mounted on a ground plane were very closely spaced in [214] and obtained an endfire realized gain of 8.81 dBi at 450 MHz. The LP ESA shown in Fig. 11 consisted of three EAD elements. Basically an EAD NFRP antenna (driven and NFRP elements) integrated with a EAD parasitic reflector. Two variations of this design were reported [215]. One prototype operated around 0.96 GHz with $ka = 0.76$ and its reflector separated from the tightly coupled pair by approximately $\lambda/10$ at the upper frequency of its 9.4% FBW_{10dB}, 1.02 GHz. Its radiation efficiency (RE) was greater than 93% and its peak broadside directivity (along the axis of the system) was 5.05 dB with a 11.4 dB FTBR. The second was $ka = 0.5$ version of the first with a slightly smaller profile operating around 1.1 GHz with a narrower 2.3% FBW_{10dB}. The peak broadside directivity was 4.2 dB with a 5.8 dB FTBR. A related CP ESA [216] consisted of a driven crossed-dipole loaded with NFRP elements and a similarly shaped cross-dipole reflector. Its prototype had $ka = 0.71$ and a $\lambda/15$ profile with a 10.56% 3-dB AR bandwidth centered around 1.47 GHz. It had a broadside gain was 2.31 dBic with a FTBR of 6.4 dB and a 80% average RE value at 1.39 GHz.

A pattern reconfigurable version of the spiral-shaped system was reported in [217]. A polarization reconfigurable version of the EAD-based system shown in Fig. 11(a) is reported in [218]. With diodes integrated into its driven element, it achieves four polarization states, 2 LP and 2 CP with peak realized gains around 3 dBic and greater than 10 dB FTBR and 70% RE values.

A 300 MHz NFRP EAD antenna was integrated with a slot-modified parasitic copper disk to obtain an electrically small system with a high directivity and a large FTBR in [219]. The EAD NFRP element acted as the director. The slot-modified disk acted as the reflector. They were separated by $\lambda/10$. The system radiated a broadside unidirectional cardioid pattern with significant directivity and an increase of the FTBR value relative to the EAD antenna alone. It had a high radiation efficiency, but very small FBW_{10dB}, $< 1.0\%$. In order to achieve more bandwidth, the parasitic disk was augmented with NIC-based capacitors. A wider directivity bandwidth was achieved [165]. Both the EAD element and the parasitic disk were later augmented, respectively, with a NIC-based inductor and NIC-based capacitors [164]. This 300 MHz NF-based ESA is illustrated in Fig. 11(b). It had $ka = 0.5$ and attained peak directivities greater than 6.3 dB with larger FTBR values > 20 dB and RE values $> 84\%$ over a much larger realized gain bandwidth, $> 10\%$. It was the first example of an ESA that overcame all of the conventional tradeoffs, i.e., it was efficient and had a large bandwidth with high peak directivity and FTBR values over it.

5.2. Huygens Dipole Antennas

Much recent work to achieve ESAs with higher directivity has been focused on Huygens sources. A Huygens source is actually well-known originally from reflector antenna developments [4]. A crossed electric and magnetic dipole combination located at the focal point of a parabolic reflector will induce currents on its surface that are parallel everywhere leading to cross-
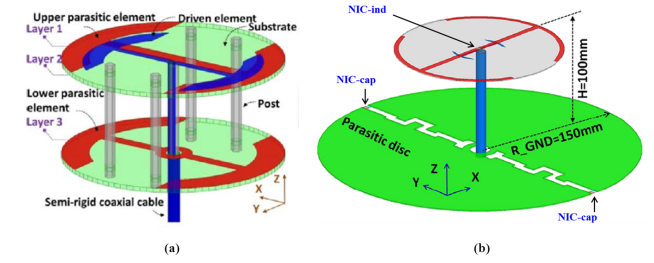

Figure 11: Quasi-Yagi NFRP ESAs. (a) Broadside radiating passive LP system. [215]. (b) Broadside radiating NF-augmented LP system [164].

polarization free far-field behavior.

The magneto-electric antennas that originated in the mid-2000's [220] are nicely reviewed in [221]. While the electromagnetics is the same, they have been described in terms of complementary sources. A large number of other authors have reported modifications and improvements of the original design, e.g., [222, 223]. They are distinguished from the electrically small systems to be described next in that they are on the order of $\lambda/2$ in size. Recent works have discussed a miniaturized version by included a CLL-based metamaterial into the configuration [224] and a reconfigurable system [225].
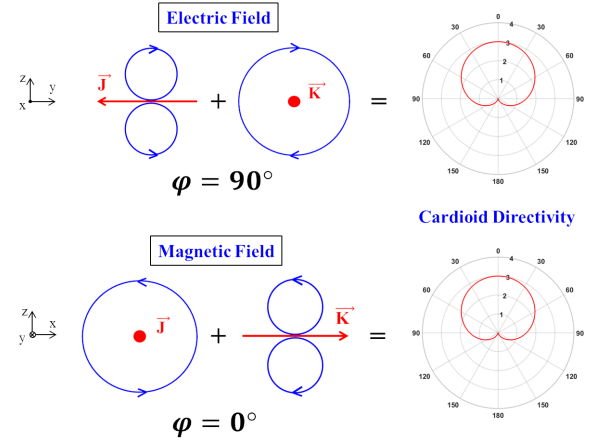

Figure 12: The Huygens radiation physics of a pair of balanced, in-phase, orthogonally oriented, infinitesimal electric and magnetic dipoles in free space.

The NFRP Huygens dipole antennas (HDAs) consist of a driven element and orthogonal electric and magnetic NFRP elements. As shown in Fig. 12, when the equivalent electric and magnetic currents arising from the driven antenna exciting the NFRP elements are properly balanced, they produce a unidirectional cardioid pattern [226, 227]. The direction of the peak directivity follows from the right-hand rule of the electric current direction crossed with the magnetic one.

The initial NFRP ESA was the endfire planar LP design shown in Fig. 13(a) [228]. Its electrical size was $ka = 0.46$, and

it was resonant at 1.475 GHz. It was designed with two 0.7874 mm thick Rogers Duroid^{TM} 5880 disks and the subsequent three copper layers. A transmission line oriented along the x-axis feeds a dipole antenna oriented along the z-axis on the middle layer. The dipole excites an electric EAD NFRP element printed on one outside surface that is oriented parallel to the z-axis and two magnetic CLL-based NFRP protractor elements printed on the other one whose dipole moments are oriented parallel to the y-axis. As shown, the radiated cardioid pattern had its peak directivity, 4.50 dB, along the +x-axis at $f_{res} = 1.54$ GHz and had a 17.1 dB FTBR value. The overall (RE) efficiency was 85.9% (86.6%). The unidirectional emitter shown in Fig. 10(a) is of a similar endfire HDA nature.

The first broadside radiating HDA is shown in Fig. 13(b). It also consisted of two of the same copper-clad substrates. A coax-fed dipole is printed on the bottom surface of the lower one; the EAD NFRP element is printed on the upper one. Two 3D copper CLL NFRP elements lie on the top surface of the bottom substrate. The gap at the center of the EAD is traversed with an inductor. The offset gaps of the CLLs are traversed with capacitors. The resonance frequency was 299.17 MHz and its $ka = 0.45$ with a 87.9% RE value. It was very low profile, the overall height being $\sim \lambda_{res}/78$. The maximum directivity of this LP HDA was 4.98 dB with the corresponding FTBR value being 17.64 dB. The first realization of the broadside radiating LP HDA had a different but analogous design [229]. A split EAD element was combined with the CLL element and driven by a coax-fed dipole. The prototype was low-profile with its height being $\sim \lambda_{res}/20$ and with $ka \sim 0.64$ at 1.50 GHz. Its peak directivity was 4.70 dB with the corresponding FTBR being 16.92 dB. The RE value was 71.6%. The cross-polarization value was smaller than -33 dB.
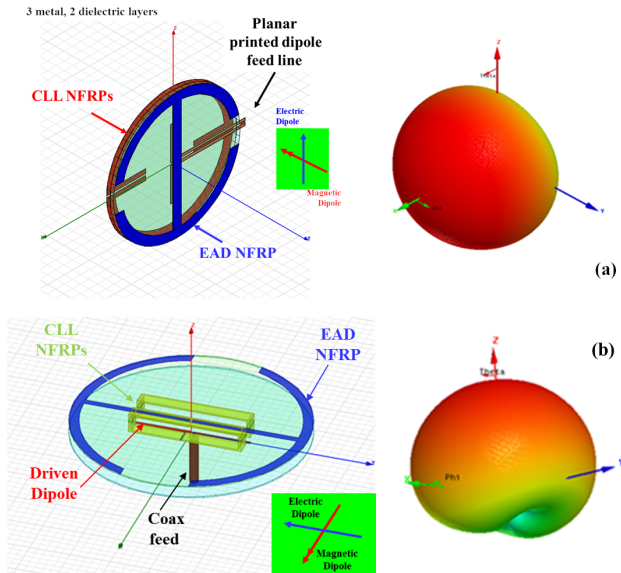
the delicate balance needed between the electric and magnetic resonators, the bandwidths of these HDA systems are narrow. The measured FBW_{10dB} of the prototype was 0.62%, i.e., a 9.3 MHz, –10-dB impedance bandwidth. As a consequence, its design was modified to achieve a better passive performance and the lumped elements were replaced with NIC versions. The resulting NF-augmented HDA had a FBW that was 10 times larger [170]. Most recently the preliminary results of a frequency-agile self-oscillating NF Huygens radiator were presented that has a measured 1:2 bandwidth, from 30 to 60 MHz [189].

A different endfire HDA was reported in [230]. It also was a two Rogers Duroid^{TM} 5880 substrate layer design. A printed spiral acted as the magnetic NFRP element. Meander-line inductor-loaded electric dipole driven and NFRP elements completed the design. It had $ka = 0.47$ at the ISM-band frequency, 0.916 MHz, and was very low profile with a height of $\lambda_{res}/103$. The directivity was 4.66 dB and an RE of 66.4%. Its FBW_{10dB} was 1.65%. Another broadside radiating HDA was reported in [231] that evolved from [229]. Two complementary spiral resonators (CSRs) and a CLL structure were used as the electric and magnetic dipoles, respectively.

A CP HDA was developed in [232]. It is illustrated in Fig. 14. It consists of two orthogonal pairs of EAD-CLL NFRP elements driven by a coax-fed crossed dipole. The electrically small ($ka = 0.73$) prototype operated at 1584 MHz. It was a low profile design with its height being $\sim \lambda_{res} / 25$. The measured peak realized gain was 2.7 dBic with a 17.7 dB FTBR value and a 68% RE value. In a similar manner to the introduction of multiple EAD and CLL elements into an electrically small package, a variety of yet more complex, multifunctional HDA-based systems have been realized. A two LP, one band system was reported in [233]. A dual band LP system was reported in [234]. A two port, dual CP system was reported in [235].
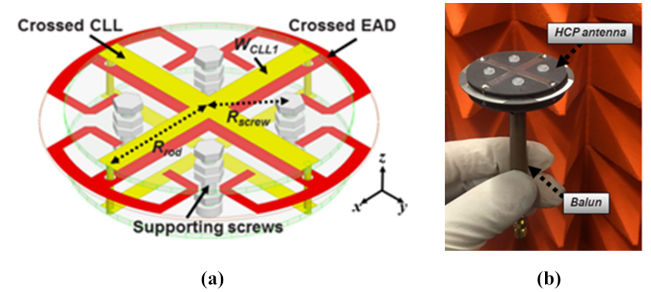

Figure 13: Huygens dipole antenna configurations. (a) Endfire radiating [228]. (b) Broadside radiating [226].

Note that the FBW_{10dB} of Fig. 13(a) was 1.57%. Similarly, the FBW_{10dB} of Fig. 13(b) was 0.20%. Because of

Figure 14: CP Huygens dipole antenna. (a) HFSS model. (b) Prototype with a bazooka balun attached for the accurate measurements. [232].

5.3. Additional Reported ESAs

As previously noted, ESAs have attracted significant interest in the antennas and propagation community and beyond. Whether you like or dislike "metamaterials (MTMs)", the fact is that they have caused a true disruption in the way that many researchers view artificial materials and think about and understand the

physics and engineering associated with electromagnetic-based radiating and scattering systems. Over time, those insights may be the most important contribution that the MTM frenzy has made. As with the already noted examples, they have impacted numerous ESA designs.

Nevertheless, there are many miniaturized antenna systems that have been conceived and explained with conventional approaches. The four-arm spherical helix antenna [25] is an excellent example from the first decade of this century. Another is the omnidirectional monopole-driven slot antenna [236]. This antenna was further showcased in the measurement analysis and campaign in [237]. A very important aspect of this work is that it nicely emphasizes the difficulties associated with measuring ESAs and provides reasons why they occur and the means to mitigate them. The list of potential problems, e.g., currents on measurement cables, misalignment of the surface normal, and polarization mismatch, is rather daunting. You will notice sleeve (bazooka) baluns in the prototype pictures herein which were necessary to help ensure accurate measured results.

As one moves to higher frequencies, these measurement difficulties increase. Discrepancies between simulated and measured results are most often predominantly blamed on fabrication and assembly errors, especially when the antenna under test (AUT) is simply put into a commercial test range and a button is pushed. While the ESA measurement demands of reviewers continue to be unrelenting, i.e., "no measurements, no publication", this topic has received little attention in the literature despite its importance. It deserves more consideration.

An ESA constructed as a driven monopole coupled to a custom-designed parasitic was developed in [238] for hearing-instruments. A meander dipole-based ESA was tailored for a RFID-based pressure sensor in [239] for glaucoma monitoring. Many other more conventional ESAs have been developed for a variety of medical related applications [240]. They all have important societal benefits.

While there are a vast number of compact/small antenna articles published indicating MTMs as being part of the radiating/receiving structures and none are actually present, there are others that are intimately connected to metamaterial-inspired concepts if one were to examine them closely. For example, the patch antenna in [241] was made small using a shorting pin and a defected ground structure (DGS) (i.e., DGSs evolved originally from electromagnetic bandgap (EBG) structures, which have often been identified as MTMs [41]). The interesting NFRP ESA developed in [242] is close in design to a 2D magnetic EZ antenna [102]. The RFID antennas considered in [243] involve a driven dipole coupled to a NFRP CLL element. The LC resonators loading a planar inverted-F antenna considered in [244] are well-known MTM unit cells. Directly driving 2D split-ring resonators (SRRs) led to interesting performance characteristics in [245]. Directly driving 3D SRRs led to the excitation of both electric and magnetic responses and an attractive quasi-isotropic ESA in [246]. Does it really matter whose favorite terminology is used to explain an antenna's operation if it is actually correct and helps a reader understand it? Absolutely not! What is really important is if the antenna does what is intended, has good performance characteristics, and has been described adequately for a reader to understand its operation

and to be able to reproduce the reported results.

6. Forward Looking ESA Applications

Given the anticipated demand for efficient, multifunctional, compact wireless devices for AWE-inspired applications, there are many opportunities for the development of novel practical ESAs for current fifth generation (5G) and evolving 6G and beyond systems. However, to make significant progress, multidisciplinary approaches involving not only further electromagnetic discoveries, but also unfolding material, circuit and measurement advances must be cultivated and nourished. Several topics that my team and collaborators are currently investigating are discussed below. They are but a tiny subset of the multitude of possibilities open to the antennas and propagation communities.

6.1. WPT and Rectennas

It is expected that AWE wireless and electronic devices have the potential to revolutionize many aspects of human life. They are being employed not only in consumer areas like communications, personal entertainment, smart homes, intelligent transportation systems, and smart cities, but also for security and health-care applications. However, the lack of very compact, long-lasting portable power sources has hindered the deployment of many IoT concepts, e.g., current battery and supercapacitor systems are too large, too heavy, or too short-lived. Consequently, wireless power transfer (WPT) technologies (e.g., also termed microwave power transmission (MPT) when restricted to microwave frequencies) have become a major trend to overcome this issue.

WPT systems negate the need for heavy, bulky, short-lived batteries and for their replacement, particularly in devices embedded in the human body or in structural materials such as in building and tunnel walls or bridge road beds. Moreover, they are environmentally friendly in the context that they avoid the need to dispose of those short-lived batteries. Furthermore, many WPT-enabled devices can be powered simultaneously from the same source. The recent pursuits of the IoT paradigm have led to the intense development of a variety of WPT technologies [247, 248].

WPT comes in many forms: near-field, mid-range and far-field systems. I will emphasize only the far-field systems. There are two main approaches to wirelessly powering devices remotely and robustly over long distances. One exploits already available ambient electromagnetic resources through wireless energy harvesting (WEH), i.e., unintentional WPT or energy recycling, which is discussed nicely, e.g., in [249–251]. Because the magnitudes of the transferred unintentional wireless power are small, WEH takes advantage of many existing frequency bands and necessarily requires broadband or multi-band antennas to capture as much of the available spectrum as is possible.

The other WPT approach is intentional WPT in which sources radiate fields at specified frequencies to wirelessly power a device. Intentional WPT aims to transfer as much power as possible from the wireless source to the targeted devices. Far-field WPT has a long history dating back into the

1960's. There are several very nice reviews of the past and recent developments [252–260].

A major component of any far-field WPT system is a rectenna, i.e., a receiving antenna integrated with a rectifying circuit to convert the incident electromagnetic (AC) power into DC power. Narrowband operation within specific frequency bands, particularly the industrial, scientific, and medical (ISM) bands, is quite common. However, the realization of high performance, ultra-compact (electrically small) rectennas, i.e., the antenna-rectifying circuit combination, is challenging. While a majority of IEEE publications on WEH and WPT have been associated with the microwave engineering community, a variety of electromagnetic analyses have also been reported. For instance, the theoretical bounds on the power transfer efficiency (PTE) and those associated with practical antennas has been studied, e.g., [261, 262]. Reviews of the key components of rectenna systems and their design requirements can be found, e.g., in [263, 264]. Reviews of antennas for microwave [265] and millimeter-wave [266] WEH and WPT, as well as the applications of metasurfaces to WEH and WPT [267, 268], have very recently appeared.

IoT devices such as sensors, communication devices, and RFID (radio frequency identification) tags require a single rectenna that is electrically small, but has a large energy capture capacity. Consequently, the HDA systems with their cardioid-shaped radiation patterns are notably advantageous. They acquire the maximum amount of power from their driving sources while not wasting power radiated in the opposite direction. A CP system has notable advantages over a LP one in certain scenarios in which the orientation of the rectenna is not guaranteed and the WPT source is either a LP or CP system.

Several of the initial metamaterial-inspired ESAs were transformed into rectennas by integrating rectifying circuits with them. Both electric [269] and magnetic [270] NFRP antenna prototypes demonstrated their predicted performance characteristics. Moreover, the NFRP HDA systems discussed above were recently adapted to realize electrically small ($ka < 0.77$) and low-profile, $0.04\,\lambda_0$, linearly (LP) and circularly (CP) polarized WPT rectennas at 915 MHz in the ISM band [271]. They too were facilitated by the seamless integration of highly efficient rectifiers, i.e., the RF signal to DC power conversion circuits, with the LP and CP HDAs. Their optimized prototypes have cardioid, very wide broadside radiation patterns, and effective capture areas larger than their physical size. Experimental results verified that they achieved a measured 89% and 82% peak AC-to-DC conversion efficiency, respectively, effectively confirming their simulated results.

One important lesson learned with those early electrically small rectenna systems was that the NFRP designs could be modified so that the antenna was matched directly to the rectifier without any intervening matching network, significantly improving their conversion efficiencies. While this aspect of the NFRP design approach was employed in the LP HDA system in [271] to attain its high conversion efficiencies, the original CP HDA rectenna design could not be tuned to be matched directly to the rectifier. The power lost to the necessary matching element was remedied in [272]. By changing the driven dipole to a more inductive form, the antenna was matched directly

to the rectifier and the system reached a maximum conversion efficiency of 90.6%. The effectiveness of directly matching the receiving antenna to the rectifier in both WPT and WEH rectenna systems was also emphasized in [273]

The advantage of the NFRP paradigm to facilitate the presence of orthogonal LP HDA systems simultaneously as illustrated in Fig. 14 was further explored for a simultaneous wireless information and power transfer (SWIPT) in [274]. SWIPT is currently being investigated in a wide range of different systems for both civil and industrial applications [260, 275]. It is one aspect of the green communications concept [276]. The CP HDA antenna and HDA rectenna designs guided the modifications needed to achieve a SWIPT HDA system. The prototype HDA-based SWIPT system had two integrated ports. One LP HDA pair was attached through one port to a rectifier for the WPT performance. The second, orthogonal LP HDA pair and its port were dedicated to communications. Similar performance characteristics to the LP versions of the LP HDA antenna and rectenna systems were obtained with over a 30 dB isolation between the two functions.

6.2. Wirelessly Powered Sensors

The next generation of sensors and control systems will be embedded in the AWE-inspired IoT electronic devices and will be consequential if they are powered with WEH and WPT technologies [277–281]. Wirelessly powered sensors and sensor networks for monitoring the health of humans (Wireless Healthcare), crops (Smart Agriculture), buildings (Smart Buildings) and even all systems and activities associated with urban environs (Smart Cities) are but a few of the imagined applications. They all will require large scale, battery-free cooperative wireless sensor networks. The HDA rectennas coupled with sensors are exceptional candidates as nodes for these systems.

Two electrically small rectenna-based wirelessly powered light and temperature sensors were developed in [282] that operate at 915 MHz in the 902–928 MHz ISM bands. One was a NFRP EAD antenna that was seamlessly integrated without any matching network with a highly efficient sensor-augmented rectifier. Its prototype was electrically small with $ka = 0.47$ at its resonance frequency, 906 MHz; was very thin (a single piece of copper-clad substrate); and its peak realized gain was 1.27 dBi. Because the system acts as an electric dipole, its omnidirectional property is ideal for capturing incident AC wireless power from any azimuthal direction and converting it into DC power. Both a photocell as the light sensor and a thermistor as the temperature sensor were demonstrated. The resistive properties of the photocell and thermistor changed the rectifier's output voltage level; an acoustic alarm was activated once a threshold value was attained. A peak 90% AC-to-DC conversion efficiency was obtained and its omnidirectional pattern was confirmed.

A LP version of the three layer electrically small, low-profile NFRP HDA shown in Fig. 14 was designed and similarly integrated with the same light- and temperature-sensor-augmented rectifiers. Its prototype had $ka = 0.73$ at its resonance frequency, 908 MHz, and was low profile with its height being $\lambda_{res} / 25$. Its broadside realized gain cardioid pattern had a 3.8 dBi peak value, more than 3 dB higher than the EAD value. The measured

peak AC-to-DC conversion efficiency was 88%.

Measurements of the prototypes of both the light-sensor and temperature-sensor augmented omni- and unidirectional rectenna systems confirmed their predicted performance characteristics. Wireless powering of both the sensor and alarm systems was demonstrated. The omnidirectional nature of the EAD-based sensors is ideal, for example, for ceiling mounted systems in long galleries in a museum. The unidirectional nature of the HDA-based sensors make it very suitable, for example, for surface-mounted applications, e.g., as temperature and light sensors on a wall in an office building or even on wine barrels resting in a cavern. As demonstrated in [227], the NFRP HDA design can be modified for placement on the surface of such dielectrics and still maintain its unidirectional performance characteristics.

A single Rogers Duroid^{TM} 5880 substrate version of the LP NFRP HDA shown in Fig. 15 was developed recently and integrated with the same sensor-augmented rectifiers [283]. Like the original endfire HDA [228], this ultra-thin rectenna system had a large electromagnetic wave capture capability and achieves nearly complete conversion of the incident energy into DC power. The HDA prototype has a realized gain of 4.6 dBi and a half power beamwidth (HPBW) of 134°. The entire rectenna is electrically small with $ka = 0.98$; is low cost and easy to fabricate; and has a measured 88% peak AC-to-DC conversion efficiency. As discussed in [254], large-scale rectenna arrays are usually implemented to capture larger amounts of power. This ultra-thin HDA system is an attractive candidate for a multi-element HDA-based rectenna array. Such a system is currently under development.
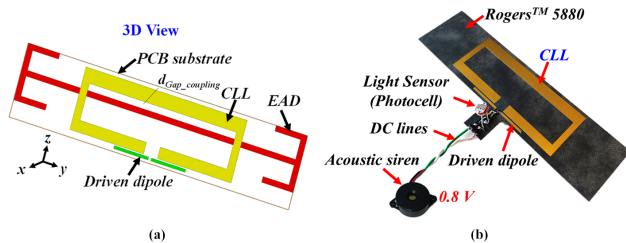

Figure 15: Ultra-thin NFRP HDA WPT system. (a) Antenna alone. (b) Antenna augmented with the sensor. [284]

6.3. Pregtronics

The concept of integrating antennas into structural materials has many applications for sensor networks and communication systems. Incorporating such electromagnetic systems into, for example, the actual bodies of land, sea and space vehicles as well as in buildings, bridges, and tunnels, one could monitor many different properties of those structures and the environments in which the operate, as well as perform their electromagnetic functions. It becomes much more than an antenna problem. It necessitates the co-design of the antenna with the materials with further adjustments in the design and implementation as the materials and fabrication processes occur and evolve.

For instance, multifunction, conformal load-bearing antenna structures offer unique structural weight savings and aerodynamic advantages in composite aerospace platforms. Many aircraft communications systems fall within the HF to UHF bands. Efficient antennas in those ranges are physically large and are generally found in the form of blade/surface monopole and/or lone wire antennas. With the advent of new antenna technologies such as the NFRP ESAs, the ability to seamlessly integrate their passive and active versions into aerospace platforms has become increasingly important. They have the key capability to be downsized for integration into small aerospace platforms. This is particularly interesting in the case of smaller unmanned aerial systems (e.g., drones) where there are significant internal volume and weight restrictions [285, 286].

A version of the EAD ESA [286] and versions of the electronics that would be needed for its NF-augmentation [285] have been developed for use in a grade of composites called "pre-impregnated" (pre-preg) materials. These pre-preg materials differ from traditional textiles in that they contain a B-staged epoxy resin that must be baked in an autoclave at temperatures greater than 170° C, and under pressures upward of 700 kPa to achieve their maximum strength. Before this curing process, they can be conformally molded to any surface. Carbon fiber reinforced plastics used in tennis rackets and bicycles are now everyday examples of these composite materials.

The antenna consisted of a differentially fed dipole element integrated with a NFRP EAD element. To achieve good matching when the antenna was in situ, a meanderline-loaded version of the dipole element was found to be necessary. The system was designed and tested at the arbitrary frequency of 300 MHz. Three ESA cases were investigated to ascertain the performance of the manufacturing techniques and material properties used to build them, as well as their performance characteristics. Photos of their prototypes are shown in Fig. 16. Uniquely, an embroidered conductive thread and a new carbon fiber based, non-woven mat were investigated for use as the conducting elements. Both cases were compared with a copper variant of the EAD antenna. The embroidered version was achieved by learning how to and then sewing the components of the antenna into the pre-preg before curing. It was the original approach and required a programmable, heavy duty sewing machine to sew the desired shapes. The veil version has since become the standard. The required shape can be laser cut out from a large piece of the non-woven mat. All three prototypes were tested. Measurements confirmed that both the non-woven mat and the embroidered versions of the EAD antennas performed similarly to the copper version [286].

Microwave pre-preg electronics, i.e., "pregtronics", was similarly established originally with embroidered transmission line studies and then by incorporating an ultrawideband (UWB) amplifier as the main component of a microwave circuit [285]. Although only a simple UWB microwave amplifier-based circuit was demonstrated, it is clear that this pathfinder prototype circuit with its passive and active components demonstrated the hybridization of composite structures and electronics. Extending the concept to incorporate digital electronics and combining all of the pregtronic concepts with the ESAs have been considered. These co-designed pregtronic-based ESAs allow for
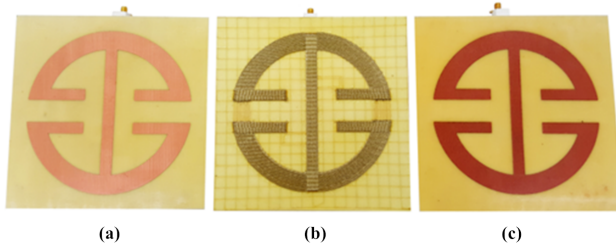
Figure 16: NFRP EAD ESA fabricated in a pre-preg structural composite material. (a) Copper version. (b) Embroidered version. (c) Veil version. [286]

the development of smart sensing, conformal structures/skins which would offer a significant advantage for efficiently utilizing the limited volume available on unmanned aerial vehicles (UAVs) and other mobile platforms.

6.4. Millimeter-wave Designs

One evolutionary technology in 5G cellular systems that is finely happening is the use of the millimeter (mmWave) frequency spectrum to realize the high data rates and system capacities that have been forecast to meet the evergrowing performance demands of consumers. Experimental results have proved that the 28 GHz frequency band is a suitable band for the initial rollouts of some mobile terminals. While much of the chatter about 5G antenna systems has been focused on millimeter-wave arrays, compact antennas continue to be in demand for many IoT applications.

Both LP and CP NFRP HDA ESAs have been developed for the 28 GHz band [287]. The LP model and its prototype are shown in Fig. 17(a). Only simulations of the CP model were provided. The use of both the LP and CP systems for on-body use were evaluated and it was demonstrated that the body had little effect on their electromagnetic performance characteristics. The potential of these HDA systems for on-body SWIPT applications is currently being investigated.

Omnidirectional CP (OCP) antennas with lower gain are expected to be the most suitable candidates for general device-to-device (D2D) applications in 5G wireless systems. They have much larger radiation coverage and, hence, enable diverse communication links among multi-users. An 28 GHz OCP ESA was realized in [288]. The model and its prototype are shown in Fig. 17(b). Instead of the electric and magnetic dipole elements being orthogonal, the balanced pair are parallel in this OCP design. It is believed to be a very good candidate for D2D communication applications.

As one can see from their photos, these 28 GHz ESAs are really tiny. While it is anticipated that electrically small versions of any antenna system will continue to be desired even as the operating frequencies increase, their physical sizes may be small enough for many applications. Moreover, the highly directive beams necessary for a variety of 5G and beyond millimeter-wave applications does necessitate arrays. Several examples of end-fire arrays of HDAs in the millimeter-wave bands have been reported at 30 GHz, e.g., [289] and 60 GHz, e.g., [290]. Since it

has been shown that the NFRP HDA designs can be tailored for on-chip applications [227], arrays of them for millimeter-wave WPT (mmWPT) are currently under development.
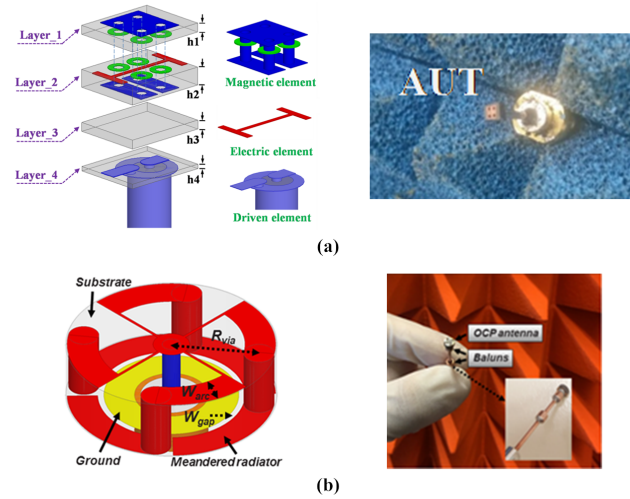

Figure 17: Millimeter-wave NFRP ESAs at 28 GHz. (a) LP HDA [287]. (b) Omnidirectional circular polarized (OCP) antenna [288].

7. Summary

While many electromagnetic, antenna and metamaterial researchers are focused on array developments for current 5G and evolving 6G beyond systems, the usefulness of efficient electrically small multifunctional, reconfigurable antennas as the ideal candidates for many of the emerging AWE-inspired IoT applications cannot be overstated. Given the concerns over how much energy will be needed to enable arrays for the anticipated 5G and beyond wireless ecosystems, any reduction of the power required by individual elements associated with high performance wireless mobile terminals and their enabling antenna systems will be welcomed. The WPT concepts discussed herein will help make 5G and beyond IoT systems more sustainable. Years of simply designing the electronic circuits and the antennas independently of each other and using intervening matching networks to enable their combinations has to stop. Co-design will only increase performance as well as save time and money. Integration of the electrically small transmitting and receiving systems directly into structural materials will decrease the weight and enhance the aesthetics of IoT devices and enable a host of applications. Co-designing compact antenna systems with novel materials to enable their functions such as reconfigurability at high millimeter-wave frequencies will have to become commonplace. Associated multidisciplinary approaches to realizing these antenna systems will become the norm as will more advanced measurement techniques to verify their performance characteristics. While you may not have been awestruck by the plethora of ESAs developed in the last two decades, I sincerely hope that the various concepts discussed and illustrated in this Overview will stimulate innovative ways

of looking at your old and new problems and, hence, prove useful to your current and future research efforts.

Acknowledgments

References

[1] L. Jofre and M. Martínez-Vázquez, *Handbook on Small Antennas*. Brussels, Belgium: EurAAP, 2012.

[2] S. R. Best, *Advances in Electrically Small Antennas*. Hoboken, NJ: John Wiley & Sons, 2012.

[3] J. L. Volakis, C.-C. Chen, and K. Fujimoto, *Small Antennas: Miniaturization Techniques & Applications*. New York, NY: McGraw Hill, 2010.

[4] C. A. Balanis, *Antenna Theory: Analysis and Design*, 4th ed. Hoboken, NJ: John Wiley & Sons, 2016.

[5] J. D. Kraus and R. J. Marhefka, *Antennas for All Applications*, 3rd ed. New York, NY: McGraw Hill, 2002.

[6] W. L. Stutzman and G. A. Thiele, *Antenna Theory and Design*. Hoboken, NJ: John Wiley & Sons, 2012.

[7] H. A. Wheeler, "Fundamental limitations of small antennas," *Proc. IRE*, vol. 35, no. 12, pp. 1479–1484, Dec. 1947.

[8] ——, "The radiansphere around a small antenna," *Proc. IRE*, vol. 47, no. 8, pp. 1325–1331, Aug. 1959.

[9] R. H. Johnston and J. G. McRory, "An improved small antenna radiation-efficiency measurement method," *IEEE Antennas Propag. Mag.*, vol. 40, no. 5, pp. 40–48, Oct. 1998.

[10] D. Heberling, M. Geissler, O. Litschke, and M. Martínez-Vázquez, "Improved radiation efficiency measurement of mobile systems and application to a novel multiband antenna," in *Proc. 2003 SBMO/IEEE MTT-S International Microwave and Optoelectronics Conference-IMOC 2003*, vol. 1. Foz do Iguacu, Brazil: IEEE, 20-23 Sep. 2003, pp. 381–386.

[11] L. J. Chu, "Physical limitations of omni-directional antennas," *J. Appl. Phys.*, vol. 19, no. 12, pp. 1163–1175, May 1948.

[12] J. S. McLean, "A re-examination of the fundamental limits on the radiation Q of electrically small antennas," *IEEE Trans. Antennas Propag.*, vol. 44, no. 5, pp. 672–676, May 1996.

[13] H. L. Thal, "New radiation Q limits for spherical wire antennas," *IEEE Trans. Antennas Propag.*, vol. 54, no. 10, pp. 2757–2763, Oct. 2006.

[14] M. Gustafsson, C. Sohl, and G. Kristensson, "Physical limitations on antennas of arbitrary shape," *Proc. Royal Soc. A*, vol. 463, no. 2086, pp. 2589–2607, Jul. 2007.

[15] A. D. Yaghjian and H. R. Stuart, "Lower bounds on the Q of electrically small dipole antennas," *IEEE Trans. Antennas Propag.*, vol. 58, no. 10, pp. 3114–3121, Oct. 2010.

[16] G. A. Vandenbosch, "Explicit relation between volume and lower bound for Q for small dipole topologies," *IEEE Trans. Antennas Propag.*, vol. 60, no. 2, pp. 1147–1152, Feb. 2011.

[17] M. Gustafsson, M. Cismasu, and B. L. G. Jonsson, "Physical bounds and optimal currents on antennas," *IEEE Trans. Antennas Propag.*, vol. 60, no. 6, pp. 2672–2681, Jun. 2012.

[18] M. Capek, L. Jelinek, P. Hazdra, and J. Eichler, "The measurable Q factor and observable energies of radiating structures," *IEEE Trans. Antennas Propag.*, vol. 62, no. 1, pp. 311–318, Jan. 2013.

[19] M. Capek, M. Gustafsson, and K. Schab, "Minimization of antenna quality factor," *IEEE Trans. Antennas Propag.*, vol. 65, no. 8, pp. 4115–4123, Aug. 2017.

[20] K. Schab, L. Jelinek, M. Capek, C. Ehrenborg, D. Tayli, G. A. Vandenbosch, and M. Gustafsson, "Energy stored by radiating systems," *IEEE Access*, vol. 6, pp. 10 553–10 568, 2018.

[21] M. Manteghi, "Fundamental limits, bandwidth, and information rate of electrically small antennas: Increasing the throughput of an antenna without violating the thermodynamic Q-factor," *IEEE Antennas Propag. Mag.*, vol. 61, no. 3, pp. 14–26, Jun. 2019.

[22] M. Gustafsson, M. Capek, and K. Schab, "Tradeoff between antenna efficiency and Q-factor," *IEEE Trans. Antennas Propag.*, vol. 67, no. 4, pp. 2482–2493, Apr. 2019.

[23] S. R. Best, "Low q electrically small linear and elliptical polarized spherical dipole antennas," *IEEE Trans. Antennas Propag.*, vol. 53, no. 3, pp. 1047–1053, Mar. 2005.

[24] ——, "Electrically small resonant planar antennas: Optimizing the quality factor and bandwidth," *IEEE Antennas Propag. Mag.*, vol. 57, no. 3, pp. 38–47, Jun. 2015.

[25] ——, "The radiation properties of electrically small folded spherical helix antennas," *IEEE Trans. Antennas Propag.*, vol. 52, no. 4, pp. 953–960, Apr. 2004.

[26] O. S. Kim, O. Breinbjerg, and A. D. Yaghjian, "Electrically small magnetic dipole antennas with quality factors approaching the Chu lower bound," *IEEE Trans. Antennas Propag.*, vol. 58, no. 6, pp. 1898–1906, Jun. 2010.

[27] H. R. Stuart and A. D. Yaghjian, "Approaching the lower bounds on Q for electrically small electric-dipole antennas using high permeability shells," *IEEE Trans. Antennas Propag.*, vol. 58, no. 12, pp. 3865–3872, Dec. 2010.

[28] D. F. Sievenpiper, D. C. Dawson, M. M. Jacob, T. Kanar, S. Kim, J. Long, and R. G. Quarfoth, "Experimental validation of performance limits and design guidelines for small antennas," *IEEE Trans. Antennas Propag.*, vol. 60, no. 1, pp. 8–19, Jan. 2011.

[29] R. W. Ziolkowski, "The directivity of a compact antenna: An unforgettable figure of merit," *EPJ Appl. Metamat.*, vol. 4, 7, 2017.

[30] P.-S. Kildal and S. R. Best, "Further investigations of fundamental directivity limitations of small antennas with and without ground planes," in *2008 IEEE Antennas and Propagation Society International Symposium*. IEEE, 2008, pp. 1–4.

[31] R. F. Harrington, "On the gain and beamwidth of directional antennas," *IRE Trans. Antennas Propag.*, vol. 6, no. 3, pp. 219–225, Jul. 1958.

[32] ——, "Effect of antenna size on gain, bandwidth, and efficiency," *J. Res. Nat. Bur. Stand*, vol. 64, no. 1, pp. 1–12, Jan.-Feb. 1960.

[33] I. Liberal, I. Ederra, R. Gonzalo, and R. W. Ziolkowski, "Induction theorem analysis of resonant nanoparticles: Design of a Huygens source nanoparticle laser," *Phys. Rev. Appl.*, vol. 1, no. 4, 044002, May 2014.

[34] R. C. Hansen, "Fundamental limitations in antennas," *Proc. IEEE*, vol. 69, no. 2, pp. 170–182, Feb. 1981.

[35] ——, "Some new calculations on antenna superdirectivity," *Proc. IEEE*, vol. 69, no. 10, pp. 1365–1366, Oct. 1981.

[36] C. W. Oseen, "Die einsteinsche nadelstichstrahlung und die maxwellschen gleichungen," *Annalen der Physik*, vol. 374, no. 19, pp. 202–204, 1922.

[37] R. W. Ziolkowski, "Using Huygens multipole arrays to realize unidirectional needle-like radiation," *Phys. Rev. X*, vol. 7, no. 3, 031017, Jul. 2017.

[38] D. Margetis, G. Fikioris, J. M. Myers, and T. T. Wu, "Highly directive current distributions: General theory," *Phys. Rev. E*, vol. 58, no. 2, p. 2531, 1998.

[39] M. Gustafsson and S. Nordebo, "Optimal antenna currents for Q, superdirectivity, and radiation patterns using convex optimization," *IEEE Trans. Antennas Propag.*, vol. 61, no. 3, pp. 1109–1118, Mar. 2013.

[40] S. Arslanagić and R. W. Ziolkowski, "Highly subwavelength, superdirective cylindrical nanoantenna," *Phys. Rev. Lett.*, vol. 120, no. 23, 237401, Jul. 2018.

[41] N. Engheta and R. W. Ziolkowski, *Metamaterials: Physics and Engineering Explorations*. Hoboken, NJ: John Wiley & Sons, 2006.

[42] G. V. Eleftheriades and K. G. Balmain, *Negative-refraction Metamaterials: Fundamental Principles and Applications*. Hoboken, NJ: John Wiley & Sons, 2005.

[43] C. Caloz and T. Itoh, *Metamaterials: Transmission Line Theory and Microwave Applications: The Engineering Approach*. Hoboken, NJ: John Wiley & Sons, 2006.

[44] R. W. Ziolkowski, P. Jin, and C.-C. Lin, "Metamaterial-inspired engineering of antennas," *Proc. IEEE*, vol. 99, no. 10, pp. 1720–1731, Oct. 2011.

[45] C. Caloz, "Metamaterial dispersion engineering concepts and applications," *Proc. IEEE*, vol. 99, no. 10, pp. 1711–1719, Oct. 2011.

[46] J. L. Volakis and K. Sertel, "Narrowband and wideband metamaterial antennas based on degenerate band edge and magnetic photonic crystals," *Proc. IEEE*, vol. 99, no. 10, pp. 1732–1745, Oct. 2011.

[47] Y. Dong and T. Itoh, "Metamaterial-based antennas," *Proc. IEEE*, vol. 100, no. 7, pp. 2271–2285, Jul. 2012.

[48] M. Durán-Sindreu, J. Naqui, F. Paredes, J. Bonache, and F. Martín, "Electrically small resonators for planar metamaterial, microwave circuit and antenna design: A comparative analysis," *Appl. Sci.*, vol. 2, no. 2, pp. 375–395, Apr. 2012.

[49] E. J. Rothwell and R. O. Ouedraogo, "Antenna miniaturization: definitions, concepts, and a review with emphasis on metamaterials," *J. Electromagn. Waves Appl.*, vol. 28, no. 17, pp. 2089–2123, 2014.

[50] R. W. Ziolkowski and A. D. Kipple, "Application of double negative materials to increase the power radiated by electrically small antennas," *IEEE Trans. Antennas Propag.*, vol. 51, no. 10, pp. 2626–2640, Oct. 2003.

[51] R. W. Ziolkowski and A. Erentok, "Metamaterial-based efficient electrically small antennas," *IEEE Trans. Antennas Propag.*, vol. 54, no. 7, pp. 2113–2130, Jul. 2006.

[52] S. A. Arslanagić, R. W. Ziolkowski, and O. Breinbjerg, "Radiation properties of an electric Hertzian dipole located near-by concentric metamaterial spheres," *Radio Sci.*, vol. 42, no. RS6S16, Nov. 2007, dOI: 10.1029/2007RS003663.

[53] H. Mosallaei and K. Sarabandi, "Antenna miniaturization and bandwidth enhancement using a reactive impedance substrate," *IEEE Trans. Antennas Propag.*, vol. 52, no. 9, pp. 2403–2414, 2004.

[54] F. Qureshi, M. A. Antoniades, and G. V. Eleftheriades, "A compact and low-profile metamaterial ring antenna with vertical polarization," *IEEE Antennas Wireless Propag. Lett.*, vol. 4, pp. 333–336, 2005.

[55] K. Buell, H. Mosallaei, and K. Sarabandi, "A substrate for small patch antennas providing tunable miniaturization factors," *IEEE Trans. Microw. Theory Techn.*, vol. 54, no. 1, pp. 135–146, Jan. 2006.

[56] H. R. Stuart and A. Pidwerbetsky, "Electrically small antenna elements using negative permittivity resonators," *IEEE Trans. Antennas Propag.*, vol. 54, no. 6, pp. 1644–1653, Jun. 2006.

[57] A. Alù, F. Bilotti, N. Engheta, and L. Vegni, "Subwavelength, compact, resonant patch antennas loaded with metamaterials," *IEEE Trans. Antennas Propag.*, vol. 55, no. 1, pp. 13–25, Jan. 2007.

[58] K. B. Alici and E. Özbay, "Radiation properties of a split ring resonator and monopole composite," *Phys. Stat. Sol. (b)*, vol. 244, no. 4, pp. 1192–1196, Apr. 2007.

[59] E. Sáenz, R. Gonzalo, I. Ederra, J. C. Vardaxoglou, and P. de Maagt, "Resonant meta-surface superstrate for single and multifrequency dipole antenna arrays," *IEEE Trans. Antennas Propag.*, vol. 56, no. 4, pp. 951–960, Apr. 2008.

[60] M. A. Antoniades and G. V. Eleftheriades, "A folded-monopole model for electrically small NRI-TL metamaterial antennas," *IEEE Antennas Wireless Propag. Lett.*, vol. 7, pp. 425–428, 2008.

[61] F. Bilotti, A. Alu, and L. Vegni, "Design of miniaturized metamaterial patch antennas with μ-negative loading," *IEEE Trans. Antennas Propag.*, vol. 56, no. 6, pp. 1640–1647, Jun. 2008.

[62] C. Caloz, T. Itoh, and A. Rennings, "CRLH traveling-wave and resonant metamaterial antennas," *IEEE Antennas Propag. Mag.*, vol. 50, no. 5, pp. 25–39, Oct. 2008.

[63] O. S. Kim and O. Breinbjerg, "Miniaturised self-resonant split-ring resonator antenna," *Electron. Lett.*, vol. 45, no. 4, pp. 196–197, Feb. 2009.

[64] G. Mumcu, K. Sertel, and J. L. Volakis, "Miniature antenna using printed coupled lines emulating degenerate band edge crystals," *IEEE Trans. Antennas Propag.*, vol. 57, no. 6, pp. 1618–1624, Jun. 2009.

[65] I. K. Kim and V. V. Varadan, "Electrically small, millimeter wave dual band meta-resonator antennas," *IEEE Trans. Antennas Propag.*, vol. 58, no. 11, pp. 3458–3463, Nov. 2010.

[66] Y. Yu, S. He, and Z. Shen, "Electrically small omni-directional antenna of circular polarization," in *2012 IEEE International Symposium on Antennas and Propagation*, Chicago, IL, USA, 2012, pp. 1–2.

[67] H. Nakano, K. Yoshida, and J. Yamauchi, "Radiation characteristics of a metaloop antenna," *IEEE Antennas Wireless Propag. Lett.s*, vol. 12, pp. 861–863, 2013.

[68] M.-C. Tang and R. W. Ziolkowski, "A study of low-profile, broadside radiation, efficient, electrically small antennas based on complementary split ring resonators," *IEEE Trans. Antennas Propag.*, vol. 61, no. 9, pp. 4419–4430, Sep. 2013.

[69] H. Wong, K.-M. Luk, C. H. Chan, Q. Xue, K. K. So, and H. W. Lai, "Small antennas in wireless communications," *Proc. IEEE*, vol. 100, no. 7, pp. 2109–2121, Jul. 2012.

[70] S. X. Ta, I. Park, and R. W. Ziolkowski, "Crossed dipole antennas: A review," *IEEE Antennas Propag. Mag.*, vol. 57, no. 5, pp. 107–122, Oct. 2015.

[71] J.-G. Lee and J.-H. Lee, "Compact zeroth-order resonator (ZOR) antennas," *EPJ Appl. Metamat.*, vol. 6, 6, 2019.

[72] M. Alibakhshikenari, B. S. Virdee, L. Azpilicueta, M. Naser-Moghadasi, M. O. Akinsolu, C. H. See, B. Liu, R. A. Abd-Alhameed, F. Falcone, I. Huynen, T. A. Denidni, and E. Limiti, "A comprehensive survey of "metamaterial transmission-line based antennas: Design, challenges, and applications"," *IEEE Access*, vol. 8, pp. 144 778–144 808, 2020.

[73] M. A. Antoniades, H. Mirzaei, and G. V. Eleftheriades, "Transmission-line based metamaterials in antenna engineering," in *Handbook of Antenna Technologies*. Springer Singapore, 2016, pp. 377–449.

[74] H. Nakano, T. Abe, and J. Yamauchi, "Quasi-theoretical investigation of four circularly polarized metaloop antennas," *EPJ Appl. Metamat.*, vol. 6, 2, 2019.

[75] M. Casaletti, G. Valerio, O. Quevedo-Teruel, and P. Burghignoli, "An overview of metasurfaces for thin antenna applications," *C. R. Phys.*, vol. 21, no. 7-8, pp. 659–676, 2020.

[76] J. Wang, Y. Li, Z. H. Jiang, T. Shi, M.-C. Tang, Z. Zhou, Z. N. Chen, and C.-W. Qiu, "Metantenna: When metasurface meets antenna again," *IEEE Trans. Antennas Propag.*, vol. 68, no. 3, pp. 1332–1347, Mar. 2020.

[77] P. Kumar, T. Ali, and M. M. Pai, "Electromagnetic metamaterials: A new paradigm of antenna design," *IEEE Access*, vol. 9, pp. 18 722–18 751, 2021.

[78] S. Arslanagić and R. W. Ziolkowski, "Active coated nano-particle excited by an arbitrarily located electric Hertzian dipole—resonance and transparency effects," *J. Opt.*, vol. 12, no. 2, 024014, Feb. 2010.

[79] R. B. Greegor, C. G. Parazzoli, J. A. Nielsen, M. H. Tanielian, D. C. Vier, S. Schultz, C. L. Holloway, and R. W. Ziolkowski, "Demonstration of impedance matching using a mu-negative (MNG) metamaterial," *IEEE Antennas Wireless Propag. Lett.*, vol. 8, pp. 92–95, 2008.

[80] R. C. Hansen, *Electrically Small, Superdirective, and Superconducting Antennas*. Hoboken, NJ: John Wiley & Sons, 2006.

[81] R. C. Hansen and R. E. Collin, *Electrically Small, Superdirective, and Superconducting Antennas*. Hoboken, NJ: Wiley-IEEE Press, 2012.

[82] R. Ziolkowski and A. Erentok, "At and below the Chu limit: Passive and active broad bandwidth metamaterial-based electrically small antennas," *IET Microw., Antennas & Propag.*, vol. 1, no. 1, pp. 116–128, Feb. 2007.

[83] A. Erentok and R. W. Ziolkowski, "A hybrid optimization method to analyze metamaterial-based electrically small antennas," *IEEE Trans. Antennas Propag.*, vol. 55, no. 3, pp. 731–741, Mar. 2007.

[84] V. Laquerbe, R. Pascaud, A. Laffont, T. Callegari, L. Liard, and O. Pascal, "Towards antenna miniaturization at radio frequencies using plasma discharges," *Phys. Plasmas*, vol. 26, no. 3, 033509, Mar. 2019.

[85] R. W. Ziolkowski, "Metamaterials: The early years in the USA," *EPJ Appl. Metamat.*, vol. 1, 5, 2014.

[86] R. W. Ziolkowski and F. Auzanneau, "Artificial molecule realization of a magnetic wall," *J. Appl. Phys.*, vol. 82, no. 7, pp. 3192–3194, Jun. 1997.

[87] ——, "Passive artificial molecule realizations of dielectric materials," *J. Appl. Phys.*, vol. 82, no. 7, pp. 3195–3198, Jul. 1997.

[88] F. Auzanneau and R. W. Ziolkowski, "Theoretical study of synthetic bianisotropic materials," *J. Electromagn. Waves Appl.*, vol. 12, no. 3, pp. 353–370, Apr. 1998.

[89] ——, "Microwave signal rectification using artificial composite materials composed of diode-loaded electrically small dipole antennas," *IEEE Trans. Microw. Theory Techn.*, vol. 46, no. 11, pp. 1628–1637, Nov. 1998.

[90] ——, "Explicit matrix formulation for the analysis of synthetic linearly and nonlinearly loaded materials in FDTD," *Prog. Electromagn. Res.*, vol. PIER 24, pp. 139–161, 1999.

[91] ——, "Artificial composite materials consisting of nonlinearly loaded electrically small antennas: Operational-amplifier-based circuits with applications to smart skins," *IEEE Trans. Antennas Propag.*, vol. 47, no. 8, pp. 1330–1339, Aug. 1999.

[92] A. Erentok, R. W. Ziolkowski, J. A. Nielsen, R. B. Greegor, C. G. Parazzoli, M. H. Tanielian, S. A. Cummer, B.-I. Popa, T. Hand, D. C. Vier, and S. Schultz, "Low frequency lumped element-based negative index metamaterial," *Appl. Phys. Lett.*, vol. 91, no. 18, 184104, Nov. 2007.

[93] A. Erentok, R. W. Ziolkowski, J. A. Nielsen, R. B. Greegor, C. G. Parazzoli, M. H. Tanielian, S. A. Cummer, B.-I. Popa, T. Hand, D. C. Vier, and S. Shultz, "Lumped element-based, highly sub-wavelength, negative index metamaterials at UHF frequencies," *J. Appl. Phys.*, vol. 104, no. 3, 034901, Aug. 2008.

[94] D. Sievenpiper, L. Zhang, R. F. Broas, N. G. Alexopolous, and E. Yablonovitch, "High-impedance electromagnetic surfaces with a forbidden frequency band," *IEEE Trans. Microw. Theory Techn.*, vol. 47, no. 11, pp. 2059–2074, Nov. 1999.

[95] R. Coccioli, F.-R. Yang, K.-P. Ma, and T. Itoh, "Aperture-coupled patch antenna on UC-PBG substrate," *IEEE Trans. Microw. Theory Techn.*, vol. 47, no. 11, pp. 2123–2130, Nov. 1999.

[96] F. Yang and Y. Rahmat-Samii, *Electromagnetic Band Gap Structures in Antenna Engineering*. Cambridge, UK: Cambridge University Press, 2009.

[97] A. Erentok, P. L. Luljak, and R. W. Ziolkowski, "Characterization of a volumetric metamaterial realization of an artificial magnetic conductor for antenna applications," *IEEE Trans. Antennas Propag.*, vol. 53, no. 1, pp. 160–172, Jan. 2005.

[98] S. J. Franson and R. W. Ziolkowski, "Numerical studies of the interaction of time-modulated multi-gigabit sequences with metamaterial structures at millimeter-wave frequencies," *Int. J. Numer. Model.*, vol. 19, no. 2, pp. 195–213, 2006.

[99] ——, "Confirmation of zero-n behavior in a high gain grid structure at millimeter-wave frequencies," *IEEE Antennas Wireless Propag. Lett.*, vol. 8, pp. 387–390, 2008.

[100] ——, "Gigabit per second data transfer in high-gain metamaterial structures at 60 GHz," *IEEE Trans. Antennas Propag.*, vol. 57, no. 10, pp. 2913–2925, Oct. 2009.

[101] P. Jin and R. W. Ziolkowski, "High-directivity, electrically small, low-profile near-field resonant parasitic antennas," *IEEE Antennas Wireless Propag. Lett.*, vol. 11, pp. 305–309, 2012.

[102] A. Erentok and R. W. Ziolkowski, "Metamaterial-inspired efficient electrically small antennas," *IEEE Trans. Antennas Propag.*, vol. 56, no. 3, pp. 691–707, Mar. 2008.

[103] S. Yan, P. J. Soh, and G. A. E. Vandenbosch, "Compact all-textile dual-band antenna loaded with metamaterial-inspired structure," *IEEE Antennas Wireless Propag. Lett.*, vol. 14, pp. 1486–1489, 2014.

[104] J. C. Myers, P. Chahal, E. Rothwell, and L. Kempel, "A multilayered metamaterial-inspired miniaturized dynamically tunable antenna," *IEEE Trans. Antennas Propag.*, vol. 63, no. 4, pp. 1546–1553, 2015.

[105] C. Zhu, T. Li, K. Li, Z.-J. Su, X. Wang, H.-Q. Zhai, L. Li, and C.-H. Liang, "Electrically small metamaterial-inspired tri-band antenna with meta-mode," *IEEE Antennas Wireless Propag. Lett.*, vol. 14, pp. 1738–1741, 2015.

[106] J. Zhang, S. Yan, and G. A. E. Vandenbosch, "Realization of dual-band pattern diversity with a CRLH-TL-inspired reconfigurable metamaterial," *IEEE Trans. Antennas Propag.*, vol. 66, no. 10, pp. 5130–5138, 2018.

[107] L. Garcia-Gamez, L. Bernard, S. Collardey, H. Covic, R. Sauleau, K. Mahdjoubi, P. Potier, and P. Pouliguen, "Compact GNSS metasurface-inspired cavity antennas," *IEEE Antennas Wireless Propag. Lett.*, vol. 18, no. 12, pp. 2652–2656, Dec. 2019.

[108] Z. Wang, Y. Dong, and T. Itoh, "Ultraminiature circularly polarized RFID antenna inspired by crossed split-ring resonator," *IEEE Trans. Antennas Propag.*, vol. 68, no. 6, pp. 4196–4207, Jun. 2020.

[109] Z. Wang and Y. Dong, "Low-profile omnidirectional WIFI antennas with pattern reconfigurability inspired by meta-resonators," *IEEE Trans. Antennas Propag.*, vol. 68, no. 10, pp. 6935–6942, Oct. 2020.

[110] Y. Shi, Q. Zeng, Y. Shang, S. Wang, S. Zhang, T. Qiu, Y. Wu, and Q. Si, "An overview of wideband metamaterials inspired electrically small antennas," in *Proc. 2020 Cross Strait Radio Science & Wireless Technology Conference (CSRSWTC)*. Fuzhou, China: IEEE, 13-16 December 2020.

[111] R. W. Ziolkowski, "Efficient electrically small antenna facilitated by a near-field resonant parasitic," *IEEE Antennas Wireless Propag. Lett.*, vol. 7, pp. 581–584, 2008.

[112] R. W. Ziolkowski, P. Jin, J. A. Nielsen, M. H. Tanielian, and C. L. Holloway, "Experimental verification of Z antennas at UHF frequencies," *IEEE Antennas Wireless Propag. Lett.*, vol. 8, pp. 1329–1333, 2009.

[113] R. W. Ziolkowski, C.-C. Lin, J. A. Nielsen, M. H. Tanielian, and C. L. Holloway, "Design and experimental verification of a 3D magnetic EZ antenna at 300 MHz," *IEEE Antennas Wireless Propag. Lett.*, vol. 8, pp. 989–993, 2009.

[114] C.-C. Lin, R. W. Ziolkowski, J. A. Nielsen, M. H. Tanielian, and C. L. Holloway, "An efficient, low pro-file, electrically small, three-dimensional, very high frequency magnetic EZ antenna," *Appl. Phys. Lett.*, vol. 96, no. 10, 104102, 2010.

[115] J. Ng, R. W. Ziolkowski, J. S. Tyo, M. C. Skipper, M. D. Abdalla, and J. Martin, "An efficient, electrically small, three-dimensional magnetic EZ antenna for HPM applications," *IEEE Trans. Plasma Sci.*, vol. 40, no. 11, pp. 3037–3045, Nov. 2012.

[116] E. S. Ramon, J. S. Tyo, R. W. Ziolkowski, M. C. Skipper, M. D. Abdalla, J. M. Martin, and L. L. Altgilbers, "A compact multi-frequency, high power radiating system combining dual-band, electrically small magnetic EZ antennas and multi-frequency standing wave oscillator sources," *IEEE Trans. Antennas Propag.*, vol. 62, no. 6, pp. 3281–3289, Jun. 2014.

[117] E. S. Ramon, J. S. Tyo, R. W. Ziolkowski, M. C. Skipper, M. D. Abdalla, and J. Martin, "Integration and operation of an electrically small magnetic EZ antenna with a high-power standing wave oscillator source," *IEEE Antennas Wireless Propag. Lett.*, vol. 15, pp. 642–645, 2015.

[118] J. Choi, F. T. Dagefu, B. M. Sadler, and K. Sarabandi, "Low-power low-VHF ad-hoc networking in complex environments," *IEEE Access*, vol. 5, pp. 24 120–24 127, 2017.

[119] S. Lim, R. L. Rogers, and H. Ling, "A tunable electrically small antenna for ground wave transmission," *IEEE Trans. Antennas Propag.*, vol. 54, no. 2, pp. 417–421, Feb. 2006.

[120] J. Oh, J. Choi, F. T. Dagefu, and K. Sarabandi, "Extremely small two-element monopole antenna for HF band applications," *IEEE Trans. Antennas Propag.*, vol. 61, no. 6, pp. 2991–2999, Jun. 2013.

[121] J. M. Baker and M. F. Iskander, "A new design approach for electrically small high-frequency antennas," *IEEE Antennas Wireless Propag. Lett.*, vol. 14, pp. 402–405, 2015.

[122] J. Choi, F. T. Dagefu, B. M. Sadler, and K. Sarabandi, "Electrically small folded dipole antenna for HF and low-VHF bands," *IEEE Antennas Wireless Propag. Lett.*, vol. 15, pp. 718–721, 2015.

[123] K. Ghaemi, R. Ma, and N. Behdad, "A small-aperture, ultrawideband HF/VHF direction-finding system for unmanned aerial vehicles," *IEEE Trans. Antennas Propag.*, vol. 66, no. 10, pp. 5109–5120, Oct. 2018.

[124] M. R. Nikkhah, F. T. Dagefu, and N. Behdad, "Electrically-small platform-based antennas for an unmanned ground vehicle," *IEEE Trans. Antennas Propag.*, vol. 68, no. 7, pp. 5189–5198, Jul. 2020.

[125] A. Bouvy and N. Behdad, "A heuristic study of the bandwidth potential of electrically-small, platform-based antennas at the HF band," *IEEE Trans. Antennas Propag.*, vol. 69, no. 2, pp. 623–635, Feb. 2021.

[126] L. Batel, J.-L. Mattei, V. Laur, A. Chevalier, and C. Delaveaud, "Tunable magneto-dielectric material for

electrically small and reconfigurable antenna systems at VHF band," *Ceramics*, vol. 3, no. 3, pp. 276–286, 2020.

[127] K. Mekki, E. Bajic, F. Chaxel, and F. Meyer, "A comparative study of LPWAN technologies for large-scale IoT deployment," *ICT Express*, vol. 5, no. 1, pp. 1–7, 2019.

[128] G. Bianco, R. Giuliano, G. Marrocco, F. Mazzenga, and A. Mejia-Aguilar, "LoRa system for search and rescue: Path loss models and procedures in mountain scenarios," *IEEE Internet Things J.*, vol. 8, no. 3, pp. 1985–1999, Feb. 2021.

[129] R. M. Foster, "A reactance theorem," *Bell Sys. Tech. J.*, vol. 3, no. 2, pp. 259–267, 1924.

[130] W. Geyi, P. Jarmuszewski, and Y. Qi, "The Foster reactance theorem for antennas and radiation Q," *IEEE Trans. Antennas Propag.*, vol. 48, no. 3, pp. 401–408, Mar. 2000.

[131] A. J. Poggio and P. E. Mayes, "Bandwidth extension for dipole antennas by conjugate reactance loading," *IEEE Trans. Antennas Propag.*, vol. 19, no. 4, pp. 544–547, Jul. 1971.

[132] J. T. Aberle and R. Loepsinger-Romak, *Antennas with non-Foster Matching Networks*. San Rafael,CA: Morgan & Claypool Publishers, 2007, vol. 2, no. 1.

[133] J. T. Aberle, "Two-port representation of an antenna with application to non-Foster matching networks," *IEEE Trans. Antennas Propag.*, vol. 56, no. 5, pp. 1218–1222, May 2008.

[134] S. E. Sussman-Fort and R. M. Rudish, "Non-Foster impedance matching of electrically-small antennas," *IEEE Trans. Antennas Propag.*, vol. 57, no. 8, pp. 2230–2241, Aug. 2009.

[135] K.-S. Song and R. G. Rojas, "Non-Foster impedance matching of electrically small antennas," in *2010 IEEE Antennas and Propagation Society International Symposium*. IEEE, 2010, pp. 1–4.

[136] E. Ugarte-Munoz, S. Hrabar, D. Segovia-Vargas, and A. Kiricenko, "Stability of non-Foster reactive elements for use in active metamaterials and antennas," *IEEE Trans. Antennas Propag.*, vol. 60, no. 7, pp. 3490–3494, Jul. 2012.

[137] C. R. White, J. S. Colburn, and R. G. Nagele, "A non-Foster VHF monopole antenna," *IEEE Antennas Wireless Propag. Lett.*, vol. 11, pp. 584–587, 2012.

[138] Y. Fan, K. Z. Rajab, M. Munoz, and Y. Hao, "Electrically small half-loop antenna design with non-Foster matching networks," in *Proc. 2012 6th European Conference on Antennas and Propagation (EUCAP)*. Prague, Czech Republic: IEEE, 26-30 March 2012, pp. 126–129.

[139] F. Albarracín-Vargas, V. Gonzalez-Posadas, F. J. Herraíz-Martinez, and D. Segovia-Vargas, "Design method for actively matched antennas with non-Foster elements," *IEEE Trans. Antennas Propag.*, vol. 64, no. 9, pp. 4118–4123, Sep. 2016.

[140] A. M. Elfrgani and R. G. Rojas, "Biomimetic antenna array using non-Foster network to enhance directional sensitivity over broad frequency band," *IEEE Trans. Antennas Propag.*, vol. 64, no. 10, pp. 4297–4305, Oct. 2016.

[141] T.-Y. Shih and N. Behdad, "Wideband, non-Foster impedance matching of electrically small transmitting antennas," *IEEE Trans. Antennas Propag.*, vol. 66, no. 11, pp. 5687–5697, Nov. 2018.

[142] H.-C. Chen, H.-Y. Yang, C.-C. Kao, and T.-G. Ma, "Slot antenna with non-Foster and negative conductance matching in consecutive bands," *IEEE Antennas Wireless Propag. Lett.*, vol. 18, no. 6, pp. 1203–1207, 2019.

[143] J. Choi, F. T. Dagefu, B. M. Sadler, and K. Sarabandi, "A miniature actively matched antenna for power-efficient and bandwidth-enhanced operation at low VHF," *IEEE Trans. Antennas Propag.*, vol. 69, no. 1, pp. 556–561, Jan. 2021.

[144] M. Alibakhshikenari, B. S. Virdee, A. A. Althuwayb, L. Azpilicueta, N. O. Parchin, C. H. See, R. A. Abd-Alhameed, F. Falcone, I. Huynen, T. A. Denidni *et al.*, "Bandwidth and gain enhancement of composite right left handed metamaterial transmission line planar antenna employing a non foster impedance matching circuit board," *Sci. Rep.*, vol. 11, no. 1, pp. 1–11, 2021.

[145] H. Li, A. Mekawy, and A. Alù, "Beyond Chu's limit with Floquet impedance matching," *Phys. Rev. Lett.*, vol. 123, no. 16, 164102, 2019.

[146] R. E. Collin, *Foundations for Microwave Engineering*. Hoboken, NJ: John Wiley & Sons, 2007.

[147] Y. Hadad, D. L. Sounas, and A. Alù, "Space-time gradient metasurfaces," *Phys. Rev. B*, vol. 92, no. 10, 100304, 2015.

[148] A. Shaltout, A. Kildishev, and V. Shalaev, "Time-varying metasurfaces and Lorentz non-reciprocity," *Opt. Mater. Express*, vol. 5, no. 11, pp. 2459–2467, 2015.

[149] S. A. Tretyakov, "Metasurfaces for general transformations of electromagnetic fields," *Phil. Trans. Roy. Soc. A: Math. Phys. Eng. Sci.*, vol. 373, no. 2049, 20140362, 2015.

[150] N. Chamanara, Y. Vahabzadeh, and C. Caloz, "Simultaneous control of the spatial and temporal spectra of light with space-time varying metasurfaces," *IEEE Trans. Antennas Propag.*, vol. 67, no. 4, pp. 2430–2441, 2019.

[151] C. Caloz and Z.-L. Deck-Léger, "Spacetime metamaterials—Part I: General concepts," *IEEE Trans. Antennas Propag.*, vol. 68, no. 3, pp. 1569–1582, 2019.

[152] ——, "Spacetime metamaterials—Part II: Theory and applications," *IEEE Trans. Antennas Propag.*, vol. 68, no. 3, pp. 1583–1598, Mar. 2019.

[153] X. Wang, A. Díaz-Rubio, H. Li, S. A. Tretyakov, and A. Alù, "Theory and design of multifunctional space-time metasurfaces," *Phys. Rev. Appl.*, vol. 13, no. 4, 044040, 2020.

[154] A. Babakhani, D. B. Rutledge, and A. Hajimiri, "Near-field direct antenna modulation," *IEEE Micro. Mag.*, vol. 10, no. 1, pp. 36–46, Feb. 2009.

[155] K. Schab, D. Huang, and J. J. Adams, "Pulse characteristics of a direct antenna modulation transmitter," *IEEE Access*, vol. 7, pp. 30 213–30 219, 2019.

[156] ——, "An energy-synchronous direct antenna modulation method for phase shift keying," *IEEE Open J. Antnenas Propag.*, vol. 1, pp. 41–46, 2020.

[157] K. Schab, "Radiation efficiency limits in direct antenna modulation transmitters," *IEEE Antennas Wireless Propag. Lett.*, vol. 19, no. 11, pp. 1911–1915, Nov. 2020.

[158] P. Jin and R. W. Ziolkowski, "Broadband, efficient, electrically small metamaterial-inspired antennas facilitated by active near-field resonant parasitic elements," *IEEE Trans. Antennas Propag.*, vol. 58, no. 2, pp. 318–327, Feb. 2010.

[159] N. Zhu and R. W. Ziolkowski, "Active metamaterial-inspired broad-bandwidth, efficient, electrically small antennas," *IEEE Antennas Wireless Propag. Lett.*, vol. 10, pp. 1582–1585, 2011.

[160] ——, "Broad-bandwidth, electrically small antenna augmented with an internal non-Foster element," *IEEE Antennas Wireless Propag. Lett.*, vol. 11, pp. 1116–1120, 2012.

[161] ——, "Design and measurements of an electrically small, broad bandwidth, non-Foster circuit-augmented protractor antenna," *Appl. Phys. Lett.*, vol. 101, no. 2, 2012, 024107.

[162] M. Barbuto, A. Monti, F. Bilotti, and A. Toscano, "Design of a non-Foster actively loaded SRR and application in metamaterial-inspired components," *IEEE Trans. Antennas Propag.*, vol. 61, no. 3, pp. 1219–1227, 2012.

[163] N. Zhu and R. W. Ziolkowski, "Broad bandwidth, electrically small, non-Foster element-augmented antenna designs, analyses, and measurements," *IEICE Trans. Commun.*, vol. 96, no. 10, pp. 2399–2409, Oct. 2013.

[164] R. W. Ziolkowski, M.-C. Tang, and N. Zhu, "An efficient, broad bandwidth, high directivity, electrically small antenna," *Microwave Opt. Tech. Lett.*, vol. 55, no. 6, pp. 1430–1434, Jun. 2013.

[165] M.-C. Tang, N. Zhu, and R. W. Ziolkowski, "Augmenting a modified Egyptian axe dipole antenna with non-Foster elements to enlarge its directivity bandwidth," *IEEE Antennas Wireless Propag. Lett.*, vol. 12, pp. 421–424, 2013.

[166] H. Mirzaei and G. V. Eleftheriades, "A resonant printed monopole antenna with an embedded non-Foster matching network," *IEEE Trans. Antennas Propag.*, vol. 61, no. 11, pp. 5363–5371, Nov. 2013.

[167] J. Church, J.-C. S. Chieh, L. Xu, J. D. Rockway, and D. Arceo, "UHF electrically small box cage loop antenna with an embedded non-Foster load," *IEEE Antennas Wireless Propag. Lett.*, vol. 13, pp. 1329–1332, 2014.

[168] R. T. Cutshall and R. W. Ziolkowski, "Performance characteristics of planar and three-dimensional versions of a frequency-agile electrically small antenna," *IEEE Antennas Propag. Mag.*, vol. 56, no. 6, pp. 53–71, Dec. 2014.

[169] G. Fu and S. Sonkusale, "Broadband wireless radio frequency power telemetry using a metamaterial resonator embedded with non-Foster impedance circuitry," *Appl. Phys. Lett.*, vol. 106, no. 20, 203504, 2015.

[170] M.-C. Tang, T. Shi, and R. W. Ziolkowski, "Electrically small, broadside radiating Huygens source antenna augmented with internal non-Foster elements to increase its bandwidth," *IEEE Antennas Wirel. Propag. Lett.*, vol. 16, pp. 712–715, 2017.

[171] H. Jaafar, D. Lemur, S. Collardey, and A. Sharaiha, "Parametric optimization of a non-Foster circuit embedded in an electrically small antenna for wideband and efficient performance," *IEEE Trans. Antennas Propag.*, vol. 67, no. 6, pp. 3619–3628, Jun. 2019.

[172] H. Jaafar, D. Lemur, S. Collardey, and A. Sharaiha, "Parametric optimization of a non-Foster circuit embedded in an electrically small antenna for wideband and efficient performance," *IEEE Trans. Antennas Propag.*, vol. 67, no. 6, pp. 3619–3628, Jun. 2019.

[173] T. Shi, M.-C. Tang, Z. Wu, H.-X. Xu, and R. W. Ziolkowski, "Improved signal-to-noise ratio, bandwidth-enhanced electrically small antenna augmented with internal non-Foster elements," *IEEE Trans. Antennas Propag.*, vol. 67, no. 4, pp. 2763–2768, Apr. 2019.

[174] A. A. Althuwayb, M. Alibakhshikenari, B. S. Virdee, F. Falcone, and E. Limiti, "Overcoming inherent narrow bandwidth and low radiation properties of electrically small antennas by using an active interior-matching circuit," *IEEE Access*, vol. 9, pp. 20 622–20 628, 2021.

[175] M.-C. Tang and R. W. Ziolkowski, "A frequency agile, ultralow-profile, complementary split ring resonator-based electrically small antenna," *Microw. Opt. Tech. Lett.*, vol. 55, no. 10, pp. 2425–2428, Oct. 2013.

[176] M.-C. Tang, R. W. Ziolkowski, S. Xiao, M. Li, and J. Zhang, "Frequency-agile, efficient, near-field resonant parasitic monopole antenna," *IEEE Trans. Antennas Propag.*, vol. 62, no. 3, pp. 1479–1483, Mar. 2014.

[177] M.-C. Tang and R. W. Ziolkowski, "Frequency-agile, efficient, circularly polarized, near-field resonant antenna: Designs and measurements," *IEEE Trans. Antennas Propag.*, vol. 63, no. 11, pp. 5203–5209, Nov. 2015.

[178] I. V. Shadrivov, S. K. Morrison, and Y. S. Kivshar, "Tunable split-ring resonators for nonlinear negative-index metamaterials," *Opt. Express*, vol. 14, no. 20, pp. 9344–9349, Oct. 2006.

[179] P. Jin and R. W. Ziolkowski, "Low-Q, electrically small, efficient near-field resonant parasitic antennas," *IEEE Trans. Antennas Propag.*, vol. 57, no. 9, pp. 2548–2563, Sep. 2009.

[180] S. Hrabar, "First ten years of active metamaterial structures with "negative" elements," *EPJ Appl. Metamaterials*, vol. 5, p. 9, 2018.

[181] S. D. Stearns, "Non-Foster circuits and stability theory," in *Proc. 2011 IEEE International Symposium on Antennas and Propagation (APSURSI)*, Spokane, WA, USA, 2011, pp. 1942–1945.

[182] ——, "Stable band-pass non-Foster circuits," in *Proc. 2015 IEEE International Symposium on Antennas and Propagation USNC/URSI National Radio Science Meeting*, Vancouver, BC, Canada, 2015, pp. 1386–1387.

[183] J. Loncar, S. Hrabar, and D. Muha, "Stability of simple lumped-distributed networks with negative capacitors," *IEEE Trans. Antennas Propag.*, vol. 65, no. 1, pp. 390–395, Jan. 2017.

[184] C. R. White, J. W. May, and J. S. Colburn, "A variable negative-inductance integrated circuit at UHF frequencies," *IEEE Microw. Compon. Lett.*, vol. 22, no. 1, pp. 35–37, Jan. 2011.

[185] D. J. Gregoire, C. R. White, and J. S. Colburn, "Wideband artificial magnetic conductors loaded with non-Foster negative inductors," *IEEE Antennas Wireless Propag. Lett.*, vol. 10, pp. 1586–1589, 2011.

[186] S. Saadat, H. Aghasi, E. Afshari, and H. Mosallaei, "Low-power negative inductance integrated circuits for GHz applications," *IEEE Microw. Compon. Lett.*, vol. 25, no. 2, pp. 118–120, Feb. 2015.

[187] L. Vincelj, I. Krois, and S. Hrabar, "Toward self-oscillating non-Foster unit cell for future active metasurfaces," *IEEE Trans. Antennas Propag.*, vol. 68, no. 3, pp. 1665–1679, Mar. 2020.

[188] L. Vincelj, S. Hrabar, and R. W. Ziolkowski, "Non-Foster self-oscillating Huygens radiator," in *Proc. 2020 IEEE International Symposium on Antennas and Propagation USNC/URSI National Radio Science Meeting*, Montreal, Canada, 5-10 Jul. 2020, pp. 521–522.

[189] ——, "Experimental demonstration of non-Foster self-oscillating Huygens radiator," in *Proc. 14th Congress on Artificial Materials for Novel Wave Phenomena - Metamaterials 2020*, New York, NY, USA, 28 Sep.–3 Oct. 2020, pp. X–508–X–510.

[190] Y. Fan, K. Z. Rajab, and Y. Hao, "Noise analysis of broadband active metamaterials with non-Foster loads," *J. Appl. Phys.*, vol. 113, no. 23, 233905, 2013.

[191] M. M. Jacob and D. F. Sievenpiper, "Gain and noise analysis of non-Foster matched antennas," *IEEE Trans. Antennas Propag.*, vol. 64, no. 12, pp. 4993–5004, Dec. 2016.

[192] P. Jin, C.-C. Lin, and R. W. Ziolkowski, "Multifunctional, electrically small, planar near-field resonant parasitic antennas," *IEEE Antennas Wireless Propag. Lett.*, vol. 11, pp. 200–204, 2012.

[193] S. X. Ta, K. Lee, I. Park, and R. W. Ziolkowski, "Compact crossed-dipole antennas loaded with near-field resonant parasitic elements," *IEEE Trans. Antennas Propag.*, vol. 65, no. 2, pp. 482–488, Feb. 2017.

[194] P. Jin and R. W. Ziolkowski, "Multi-frequency, linear and circular polarized, metamaterial-inspired, near-field resonant parasitic antennas," *IEEE Trans. Antennas Propag.*, vol. 59, no. 5, pp. 1446–1459, May 2011.

[195] S. X. Ta, H. Choo, I. Park, and R. W. Ziolkowski, "Multiband, wide-beam, circularly polarized, crossed, asymmetrically barbed dipole antennas for gps applications," *IEEE Trans. Antennas Propag.*, vol. 61, no. 11, pp. 5771–5775, Nov. 2013.

[196] O. Turkmen, G. Turhan-Sayan, and R. W. Ziolkowski, "Single-, dual-, and triple-band metamaterial-inspired electrically small planar magnetic dipole antennas," *Microw. Opt. Tech. Lett.*, vol. 56, no. 1, pp. 83–87, Jan. 2014.

[197] S. Dakhli, H. Rmili, J.-M. Floc'h, M. Sheikh, A. Dobaie, K. Mahdjoubi, F. Choubani, and R. W. Ziolkowski, "Printed multiband metamaterial-inspired antennas," *Microw. Opt. Tech. Lett.*, vol. 58, no. 6, pp. 1281–1289, Jun. 2016.

[198] S. X. Ta, I. Park, and R. W. Ziolkowski, "Circularly polarized crossed dipole on an HIS for 2.4/5.2/5.8-GHz WLAN applications," *IEEE Antennas Wireless Propag. Lett.*, vol. 12, pp. 1464–1467, 2013.

[199] P. P. Shome, T. Khan, S. Koul, and Y. Antar, "Filtenna designs for radio-frequency front-end systems: A structural-oriented review," *IEEE Antennas Propag. Mag.*, early access, 2020, DOI:10.1109/MAP.2020.2988518.

[200] M.-C. Tang, Y. Chen, and R. W. Ziolkowski, "Experimentally validated, planar, wideband, electrically small, monopole filtennas based on capacitively loaded loop resonators," *IEEE Trans. Antennas Propag.*, vol. 64, no. 8, pp. 3353–3360, Aug. 2016.

[201] X. Chen, M. Tang, D. Yi, and R. W. Ziolkowski, "Wideband, electrically small, near-field resonant parasitic dipole antenna with stable radiation performance," *IEEE Antennas Wireless Propag. Lett.*, vol. 19, no. 5, pp. 826–830, May 2020.

[202] M. Tang, D. Li, Y. Wang, K. Hu, and R. W. Ziolkowski, "Compact, low-profile, linearly and circularly polarized filtennas enabled with custom-designed feed-probe structures," *IEEE Trans. Antennas Propag.*, vol. 68, no. 7, pp. 5247–5256, Jul. 2020.

[203] J. T. Bernhard, *Reconfigurable Antennas*. Williston, VT, USA: Morgan & Claypool, 2007.

[204] C. G. Christodoulou, Y. Tawk, S. A. Lane, and S. R. Erwin, "Reconfigurable antennas for wireless and space applications," *Proc. IEEE*, vol. 100, no. 7, pp. 2250–2261, Jul. 2012.

[205] Y. J. Guo, P. Qin, S. Chen, W. Lin, and R. W. Ziolkowski, "Advances in reconfigurable antenna systems facilitated

by innovative technologies," *IEEE Access*, vol. 6, pp. 5780–5794, 2018.

[206] M.-C. Tang, T. Shi, and R. Ziolkowski, "Electrically small uniplanar antenna with pattern-agile performance," *Electron. Lett.*, vol. 51, no. 16, pp. 1228–1229, Aug. 2015.

[207] S. Dakhli, H. Rmili, J.-m. Floc'h, M. Sheikh, K. Mahdjoubi, F. Choubani, and R. W. Ziolkowski, "Capacitively loaded loop-based antennas with reconfigurable radiation patterns," *Int. J. Antennas Propag.*, vol. 2015, 2015, 523198.

[208] M.-C. Tang, B. Zhou, and R. W. Ziolkowski, "Low-profile, electrically small, Huygens source antenna with pattern-reconfigurability that covers the entire azimuthal plane," *IEEE Trans. Antennas Propag.*, vol. 65, no. 3, pp. 1063–1072, Mar. 2017.

[209] M.-C. Tang, Y. Duan, Z. Wu, X. Chen, M. Li, and R. W. Ziolkowski, "Pattern reconfigurable, vertically polarized, low-profile, compact, near-field resonant parasitic antenna," *IEEE Trans. Antennas Propag.*, vol. 67, no. 3, pp. 1467–1475, Mar. 2018.

[210] M. Tang, Y. Chen, X. Chen, D. Mu, and R. W. Ziolkowski, "Design and testing of a simple, compact antenna with reconfigurable broadside and monopole-like patterns," *IEEE Antennas Wireless Propag. Lett.*, vol. 19, no. 6, pp. 897–901, Jun. 2020.

[211] Z. Wu, M. Tang, M. Li, and R. W. Ziolkowski, "Ultralow-profile, electrically small, pattern-reconfigurable metamaterial-inspired Huygens dipole antenna," *IEEE Trans. Antennas Propag.*, vol. 68, no. 3, pp. 1238–1248, Mar. 2020.

[212] M.-C. Tang, Z. Wu, T. Shi, and R. W. Ziolkowski, "Electrically small, low-profile, planar, Huygens dipole antenna with quad-polarization diversity," *IEEE Trans. Antennas Propag.*, vol. 66, no. 12, pp. 6772–6780, Dec. 2018.

[213] M.-C. Tang, B. Zhou, and R. W. Ziolkowski, "Flexible uniplanar electrically small directive antenna empowered by a modified CPW-feed," *IEEE Antennas Wireless Propag. Lett.*, vol. 15, pp. 914–917, 2016.

[214] S. Lim and H. Ling, "Design of electrically small Yagi antenna," *Electron. Lett.*, vol. 43, no. 5, pp. 3–4, 2007.

[215] M.-C. Tang, R. W. Ziolkowski, S. Xiao, and M. Li, "A high-directivity, wideband, efficient, electrically small antenna system," *IEEE Trans. Antennas Propag.*, vol. 62, no. 12, pp. 6541–6547, Dec. 2014.

[216] S. X. Ta, I. Park, and R. W. Ziolkowski, "Broadband electrically small circularly polarized directive antenna," *IEEE Access*, vol. 5, pp. 14 657–14 663, 2017.

[217] S. Lim and H. Ling, "Design of electrically small, pattern reconfigurable Yagi antenna," *Electron. Lett.*, vol. 43, no. 24, pp. 1326–1327, 2007.

[218] M. Tang, Q. Lin, M. Li, and R. W. Ziolkowski, "Polarization-reconfigurable Yagi-configured electrically

small antenna," *IEEE Trans. Antennas Propag.*, vol. 69, no. 3, pp. 1757–1762, Mar. 2021.

[219] M.-C. Tang and R. W. Ziolkowski, "Efficient, high directivity, large front-to-back-ratio, electrically small, near-field-resonant-parasitic antenna," *IEEE Access*, vol. 1, pp. 16–28, 2013.

[220] K.-M. Luk and H. Wong, "A new wideband unidirectional antenna element," *Int. J. Microw. Opt. Technol.*, vol. 1, no. 1, pp. 35–44, 2006.

[221] K.-M. Luk and B. Wu, "The magnetoelectric dipole – A wideband antenna for base stations in mobile communications," *Proc. IEEE*, vol. 100, no. 7, pp. 2297–2307, Jul. 2012.

[222] H.-J. Seo and A. A. Kishk, "Wideband linear and dual-polarized antenna based on Huygens' source principle," in *Proc. 2011 XXXth URSI General Assembly and Scientific Symposium*. Istanbul, Turkey: IEEE, 2011, pp. 1–4.

[223] ——, "Wideband magnetic-electric antenna with linear single or dual polarization," *Prog. Electromagn. Res.*, vol. 155, pp. 53–61, 2016.

[224] M. Li, K. Luk, L. Ge, and K. Zhang, "Miniaturization of magnetoelectric dipole antenna by using metamaterial loading," *IEEE Trans. Antennas Propag.*, vol. 64, no. 11, pp. 4914–4918, Nov. 2016.

[225] F. Wu and K. M. Luk, "A compact and reconfigurable circularly polarized complementary antenna," *IEEE Antennas Propag. Mag.*, vol. 16, pp. 1188–1191, 2017.

[226] R. W. Ziolkowski, "Low profile, broadside radiating, electrically small Huygens source antennas," *IEEE Access*, vol. 3, pp. 2644–2651, Dec. 2015.

[227] ——, "Custom-designed electrically small Huygens dipole antennas achieve efficient, directive emissions into air when mounted on a high permittivity block," *IEEE Access*, vol. 7, pp. 163 365–163 383, Jul. 2019.

[228] P. Jin and R. W. Ziolkowski, "Metamaterial-inspired, electrically small Huygens sources," *IEEE Antennas Wirel. Propag. Lett.*, vol. 9, pp. 501–505, 2010.

[229] M.-C. Tang, H. Wang, and R. W. Ziolkowski, "Design and testing of simple, electrically small, low-profile, Huygens source antennas with broadside radiation performance," *IEEE Trans. Antennas Propag.*, vol. 64, no. 11, pp. 4607–4617, Nov. 2016.

[230] S. Lee, G. Shin, S. M. Radha, J. Choi, and I. Yoon, "Low-profile, electrically small planar Huygens source antenna with an endfire radiation characteristic," *IEEE Antennas Wireless Propag. Lett.*, vol. 18, no. 3, pp. 412–416, Mar. 2019.

[231] V. Jantarachote, S. Chalermwisutkul, W. Chansumran, and W. Longcharoen, "Electrically small Huygens source antennas based on complementary spiral resonator," in *Proc. 2019 16th International Conference on Electrical Engineering/Electronics, Computer, Telecommunications*

and Information Technology (ECTI-CON), Pattaya, Thailand, 2019, pp. 752–755.

[232] W. Lin and R. W. Ziolkowski, "Electrically-small, low-profile, Huygens circularly polarized antenna," *IEEE Trans. Antennas Propag.*, vol. 66, no. 2, pp. 636–643, Feb. 2018.

[233] M. Tang, Z. Wu, T. Shi, H. Zeng, W. Lin, and R. W. Ziolkowski, "Dual-linearly polarized, electrically small, low-profile, broadside radiating, Huygens dipole antenna," *IEEE Trans. Antennas Propag.*, vol. 66, no. 8, pp. 3877–3885, 2018.

[234] M. Tang, Z. Wu, T. Shi, and R. W. Ziolkowski, "Dual-band, linearly polarized, electrically small Huygens dipole antennas," *IEEE Trans. Antennas Propag.*, vol. 67, no. 1, pp. 37–47, Jan. 2019.

[235] Z. Wu, M. Tang, T. Shi, and R. W. Ziolkowski, "Two-port, dual-circularly polarized, low-profile broadside-radiating electrically small Huygens dipole antenna," *IEEE Trans. Antennas Propag.*, vol. 69, no. 1, pp. 514–519, Jan. 2021.

[236] S. Sufyar and C. Delaveaud, "A miniaturization technique of a compact omnidirectional antenna," *Radioengineering*, vol. 18, no. 4, pp. 373–380, Dec. 2009.

[237] L. Huitema, C. Delaveaud, and R. D'Errico, "Impedance and radiation measurement methodology for ultra miniature antennas," *IEEE Trans. Antennas Propag.*, vol. 62, no. 7, pp. 3463–3473, Jul. 2014.

[238] L. Fmrch, S. H. Kvist, J. Thaysen, and K. B. Jakobsen, "Electric-coupled antenna for hearing-instrument applications," in *Proc. 2016 Loughborough Antennas Propagation Conference (LAPC)*, Loughborough, UK, 14-15 Nov. 2016, pp. 1–4.

[239] A. Faul and J. Naber, "A novel 915 MHz, RFID-based pressure sensor for glaucoma using an electrically small antenna," *Analog Integr. Circuits Signal Process.*, vol. 85, no. 1, pp. 167–180, 2015.

[240] A. Sani, M. Rajab, R. Foster, and Y. Hao, "Antennas and propagation of implanted RFIDs for pervasive healthcare applications," *Proc. IEEE*, vol. 98, no. 9, pp. 1648–1655, Sep. 2010.

[241] A. A. Salih and M. S. Sharawi, "A dual-band highly miniaturized patch antenna," *IEEE Antennas Wireless Propag. Lett.*, vol. 15, pp. 1783–1786, 2016.

[242] S. Yan and G. A. Vandenbosch, "A fully planar near-field resonant parasitic antenna," *Prog. Electromagn. Res.*, vol. 54, pp. 163–169, 2014.

[243] P. Turalchuk, I. Munina, M. Derkach, O. Vendik, and I. Vendik, "Electrically small loop antennas for RFID applications," *IEEE Antennas Wireless Propag. Lett.*, vol. 14, pp. 1786–1789, 2015.

[244] S. V. Reddy, K. Saurav, D. Sarkar, and K. V. Srivastava, "Design of compact planar inverted-F antennas loaded with LC resonators," in *Proc. 2015 IEEE UP Section Conference on Electrical Computer and Electronics (UP-CON)*, Allahabad, India, 4-6 Dec. 2015, pp. 1–5.

[245] S. Zuffanelli, G. Zamora, P. Aguilà, F. Paredes, F. Martín, and J. Bonache, "On the radiation properties of split-ring resonators (SRRs) at the second resonance," *IEEE Trans. Microw. Theory Techn.*, vol. 63, no. 7, pp. 2133–2141, Jul. 2015.

[246] J. Kim and S. Nam, "A compact quasi-isotropic antenna based on folded split-ring resonators," *IEEE Antennas Wireless Propag. Lett.*, vol. 16, pp. 294–297, 2017.

[247] L. Roselli, C. Mariotti, M. Virili, F. Alimenti, G. Orecchini, V. Palazzi, P. Mezzanotte, and N. B. Carvalho, "WPT related applications enabling Internet of Things evolution," in *Proc. 2016 10th European Conference on Antennas and Propagation (EuCAP)*, Davos, Switzerland, 11-15 April 2016, pp. 1–2.

[248] M. R. Palattella, M. Dohler, A. Grieco, G. Rizzo, J. Torsner, T. Engel, and L. Ladid, "Internet of Things in the 5G era: Enablers, architecture, and business models," *IEEE J. Sel. Areas Commun.*, vol. 34, no. 3, pp. 510–527, Mar. 2016.

[249] J. A. Hagerty, F. B. Helmbrecht, W. H. McCalpin, R. Zane, and Z. B. Popovic, "Recycling ambient microwave energy with broad-band rectenna arrays," *IEEE Trans. Microw. Theory Techn.*, vol. 52, no. 3, pp. 1014–1024, Mar. 2004.

[250] Z. Popovic, "Cut the cord: Low-power far-field wireless powering," *IEEE Microw. Mag.*, vol. 14, no. 2, pp. 55–62, Feb. 2013.

[251] C. R. Valenta and G. D. Durgin, "Harvesting wireless power: Survey of energy-harvester conversion efficiency in far-field, wireless power transfer systems," *IEEE Microw. Mag.*, vol. 15, no. 4, pp. 108–120, Jun. 2014.

[252] W. C. Brown, "The history of power transmission by radio waves," *IEEE Trans. Microw. Theory Tech.*, vol. 32, no. 9, pp. 1230–1242, Sep. 1984.

[253] B. Strassner and K. Chang, "Microwave power transmission: Historical milestones and system components," *Proc. IEEE*, vol. 101, no. 6, pp. 1379–1396, Jun. 2013.

[254] A. Massa, G. Oliveri, F. Viani, and P. Rocca, "Array designs for long-distance wireless power transmission: State-of-the-art and innovative solutions," *Proc. IEEE*, vol. 101, no. 6, pp. 1464–1481, Jun. 2013.

[255] A. Costanzo, M. Dionigi, D. Masotti, M. Mongiardo, G. Monti, L. Tarricone, and R. Sorrentino, "Electromagnetic energy harvesting and wireless power transmission: A unified approach," *Proc. IEEE*, vol. 102, no. 11, pp. 1692–1711, 2014.

[256] N. Borges Carvalho, A. Georgiadis, A. Costanzo, H. Rogier, A. Collado, and et al., "Wireless power transmission: R & D activities within Europe," *IEEE Trans. Microw. Theory Techn.*, vol. 62, no. 4, pp. 1031–1045, Apr. 2014.

[257] A. Costanzo and D. Masotti, "Smart solutions in smart spaces: Getting the most from far-field wireless power transfer," *IEEE Microw. Mag.*, vol. 17, no. 5, pp. 30–45, May 2016.

[258] Z. Popovic, "Near- and far-field wireless power transfer," in *Proc. 2017 13th International Conference on Advanced Technologies, Systems and Services in Telecommunications (TELSIKS)*, Nis, Serbia, 2017, pp. 3–6.

[259] J. G. D. Hester, J. Kimionis, and M. M. Tentzeris, "Printed motes for IoT wireless networks: State of the art, challenges, and outlooks," *IEEE Trans. Microw. Theory Techn.*, vol. 65, no. 5, pp. 1819–1830, May 2017.

[260] A. Costanzo and D. Masotti, "Energizing 5G: Near- and far-field wireless energy and data transfer as an enabling technology for the 5G IoT," *IEEE Microw. Mag.*, vol. 18, no. 3, pp. 125–136, 2017.

[261] Y. G. Kim and S. Nam, "Determination of the impedance parameters of antennas and the maximum power transfer efficiency of wireless power transfer," *IEEE Trans. Antennas Propag.*, vol. 67, no. 8, pp. 5132–5144, Aug. 2019.

[262] J. Kim, Y. Lim, and S. Nam, "Efficiency bound of radiative wireless power transmission using practical antennas," *IEEE Trans. Antennas Propag.*, vol. 67, no. 8, pp. 5750–5755, Aug. 2019.

[263] D. Surender, T. Khan, F. A. Talukdar, A. De, Y. M. Antar, and A. P. Freundorfer, "Key components of rectenna system: A comprehensive survey," *IETE J. Research*, pp. 1–27, May 2020, dOI: 10.1080/03772063.2020.1761268.

[264] N. Shinohara, "Trends in wireless power transfer: WPT technology for energy harvesting, mllimeter-wave/THz rectennas, MIMO-WPT, and advances in near-field WPT applications," *IEEE Microw. Mag.*, vol. 22, no. 1, pp. 46–59, Jan. 2020.

[265] M. Wagih, A. S. Weddell, and S. Beeby, "Rectennas for radio-frequency energy harvesting and wireless power transfer: A review of antenna design," *IEEE Antennas Propag. Mag.*, vol. 62, no. 5, pp. 95–107, Oct. 2020.

[266] ——, "Millimeter-wave power harvesting: A review," *IEEE Open J. Antennas Propag.*, vol. 1, pp. 560–578, 2020.

[267] L. Li, X. Zhang, C. Song, and Y. Huang, "Progress, challenges, and perspective on metasurfaces for ambient radio frequency energy harvesting," *Appl. Phys. Lett.*, vol. 116, no. 6, 060501, 2020.

[268] A. A. Eteng, H. H. Goh, S. K. A. Rahim, and A. Alomainy, "A review of metasurfaces for microwave energy transmission and harvesting in wireless powered networks," *IEEE Access*, vol. 9, pp. 27 518–27 539, 2021.

[269] N. Zhu, R. W. Ziolkowski, and H. Xin, "A metamaterial-inspired, electrically small rectenna for high-efficiency, low power harvesting and scavenging at the global positioning system L1 frequency," *Appl. Phys. Lett.*, vol. 99, no. 11, 2011, 114101.

[270] ——, "Electrically small GPS L1 rectennas," *IEEE Antennas Wireless Propag. Lett.*, vol. 10, pp. 935–938, 2011.

[271] W. Lin, R. W. Ziolkowski, and J. Huang, "Electrically small, low profile, highly efficient, Huygens dipole rectennas for wirelessly powering internet-of-things (IoT) devices," *IEEE Trans. Antennas Propag.*, vol. 67, no. 6, pp. 3670–3679, Jun. 2019.

[272] W. Lin and R. W. Ziolkowski, "Electrically small huygens cp rectenna with a driven loop element maximizes its wireless power transfer efficiency," *IEEE Trans. Antennas Propag.*, vol. 68, no. 1, pp. 540–545, Jan. 2020.

[273] C. Song, Y. Huang, J. Zhou, P. Carter, S. Yuan, Q. Xu, and Z. Fei, "Matching network elimination in broadband rectennas for high-efficiency wireless power transfer and energy harvesting," *IEEE Trans. Ind. Electron.*, vol. 64, no. 5, pp. 3950–3961, May 2017.

[274] W. Lin and R. W. Ziolkowski, "Electrically small Huygens antenna-based fully-integrated wireless power transfer and communication system," *IEEE Access*, vol. 7, pp. 39 762–39 769, Apr. 2019.

[275] F. Jameel, Faisal, M. A. A. Haider, and A. A. Butt, "A technical review of simultaneous wireless information and power transfer (SWIPT)," in *Proc. 2017 International Symposium on Recent Advances in Electrical Engineering (RAEE)*, Islamabad, Pakistan, 2017, pp. 1–6.

[276] H.-S. Nguyen, D.-T. Do, and M. Voznak, "Two-way relaying networks in green communications for 5G: Optimal throughput and tradeoff between relay distance on power splitting-based and time switching-based relaying SWIPT," *Int. J. Electron. Commun.*, vol. 70, no. 12, pp. 1637–1644, Dec. 2016.

[277] Z. Popović, E. A. Falkenstein, D. Costinett, and R. Zane, "Low-power farfield wireless powering for wireless sensors," *Proc. IEEE*, vol. 101, no. 6, pp. 1397–1409, Jun. 2013.

[278] H. J. Visser and R. J. M. Vullers, "RF energy harvesting and transport for wireless sensor network applications: Principles and requirements," *Proc. IEEE*, vol. 101, no. 6, pp. 1410–1423, Jun. 2013.

[279] S. Kim, R. Vyas, J. Bito, K. Niotaki, A. Collado, A. Georgiadis, and M. M. Tentzeris, "Ambient RF energy-harvesting technologies for self-sustainable standalone wireless sensor platforms," *Proc. IEEE*, vol. 102, no. 11, pp. 1649–1666, Nov. 2014.

[280] H. Khodr, N. Kouzayha, M. Abdallah, J. Costantine, and Z. Dawy, "Energy efficient IoT sensor with RF wake-up and addressing capability," *IEEE Sensors Lett.*, vol. 1, no. 6, pp. 1–4, Dec. 2017.

[281] O. Bjorkqvist, O. Dahlberg, G. Silver, C. Kolitsidas, O. Quevedo-Teruel, and B. L. G. Jonsson, "Wireless sensor network utilizing radio-frequency energy harvesting for smart building applications," *IEEE Antennas Propag. Mag.*, vol. 60, no. 5, pp. 124–136, Oct. 2018.

[282] W. Lin and R. W. Ziolkowski, "Wirelessly powered light and temperature sensors facilitated by electrically small omnidirectional and Huygens dipole antennas," *Sensors*, vol. 19, no. 9, 1998, Apr. 2019.

[283] W. Lin and R. W. Ziolkowski, "Wireless power transfer (WPT) enabled IoT sensors based on ultra-thin electrically small antennas," in *Proc. 2021 15th European Conference on Antennas and Propagation (EUCAP)*. Düsseldorf, Germany: IEEE, 22-26 March 2021.

[284] ——, "Electrically small, single-substrate Huygens dipole rectenna for ultra-compact wireless power transfer applications," *IEEE Trans. Antennas Propag.*, vol. 69, no. 2, pp. 1130–1134, Feb. 2021.

[285] T. C. Baum, R. W. Ziolkowski, K. Ghorbani, and K. J. Nicholson, "Embroidered active microwave composite preimpregnated electronics—Pregtronics," *IEEE Trans. Microw. Theory Techn.*, vol. 64, no. 10, pp. 3175–3186, Oct. 2016.

[286] ——, "Investigations of a load-bearing composite electrically small Egyptian axe dipole antenna," *IEEE Trans. Antennas Propag.*, vol. 65, no. 8, pp. 3827–3837, Aug. 2017.

[287] M.-C. Tang, T. Shi, and R. W. Ziolkowski, "A study of 28 GHz, planar, multilayered, electrically small, broadside radiating, Huygens source antennas," *IEEE Trans. Antennas Propag.*, vol. 65, no. 12, pp. 6345–6354, Dec. 2017.

[288] W. Lin, R. W. Ziolkowski, and T. C. Baum, "28 GHz compact omnidirectional circularly polarized antenna for device-to-device communications in the future 5G systems," *IEEE Trans. Antennas Propag.*, vol. 65, no. 12, pp. 6904–6914, Dec. 2017.

[289] N. Ashraf, A. R. Sebak, and A. A. Kishk, "Packaged microstrip line feed network on a single surface for dual-polarized $2^N \times 2^M$ ME-dipole antenna array," *IEEE Antennas Wireless Propag. Lett.*, vol. 19, no. 4, pp. 596–600, 2020.

[290] Y. Li and K. Luk, "A multibeam end-fire magnetoelectric dipole antenna array for millimeter-wave applications," *IEEE Trans. Antennas Propag.*, vol. 64, no. 7, pp. 2894–2904, Jul. 2016.